

RESEARCH ARTICLE

Diversification in the HIV-1 Envelope Hyper-variable Domains V2, V4, and V5 and Higher Probability of Transmitted/Founder Envelope Glycosylation Favor the Development of Heterologous Neutralization Breadth

S. Abigail Smith^{1,2}, Samantha L. Burton^{1,2}, William Kilembe³, Shabir Lakhi³, Etienne Karita⁴, Matt Price^{5,6}, Susan Allen⁷, Eric Hunter^{1,2,7}, Cynthia A. Derdeyn^{1,2,7*}

1 Yerkes National Primate Research Center, Emory University Atlanta, Georgia, United States of America, **2** Emory Vaccine Center, Emory University Atlanta, Georgia, United States of America, **3** Zambia Emory HIV Research Project, Lusaka, Ndola and Kitwe, Zambia, **4** Projct San Francisco, Kigali, Rwanda, **5** International AIDS Vaccine Initiative (IAVI), New York, New York, United States of America, **6** UCSF Department of Epidemiology and Biostatistics, San Francisco, California, United States of America, **7** Department of Pathology and Laboratory Medicine, Emory University Atlanta, Georgia, United States of America

* cderdey@emory.edu



CrossMark
click for updates

 OPEN ACCESS

Citation: Smith SA, Burton SL, Kilembe W, Lakhi S, Karita E, Price M, et al. (2016) Diversification in the HIV-1 Envelope Hyper-variable Domains V2, V4, and V5 and Higher Probability of Transmitted/Founder Envelope Glycosylation Favor the Development of Heterologous Neutralization Breadth. *PLoS Pathog* 12(11): e1005989. doi:10.1371/journal.ppat.1005989

Editor: Alexandra Trkola, University of Zurich, SWITZERLAND

Received: May 19, 2016

Accepted: October 11, 2016

Published: November 16, 2016

Copyright: © 2016 Smith et al. This is an open access article distributed under the terms of the [Creative Commons Attribution License](https://creativecommons.org/licenses/by/4.0/), which permits unrestricted use, distribution, and reproduction in any medium, provided the original author and source are credited.

Data Availability Statement: Sequences have been deposited into Genbank for public access: KX983471-KX983929 (<http://www.ncbi.nlm.nih.gov/genbank/>).

Funding: This study was funded by the National Institutes of Health (<https://www.nih.gov/>), National Institute for Allergy and Infectious Diseases (<https://www.niaid.nih.gov/>) through the following grants: R01 AI58706 (CAD), R01 AI064060 (EH), and R37 AI051231 (EH). Additional support was provided by the International AIDS Vaccine Initiative (IAVI);

Abstract

A recent study of plasma neutralization breadth in HIV-1 infected individuals at nine International AIDS Vaccine Initiative (IAVI) sites reported that viral load, HLA-A*03 genotype, and subtype C infection were strongly associated with the development of neutralization breadth. Here, we refine the findings of that study by analyzing the impact of the transmitted/founder (T/F) envelope (Env), early Env diversification, and autologous neutralization on the development of plasma neutralization breadth in 21 participants identified during recent infection at two of those sites: Kigali, Rwanda (n = 9) and Lusaka, Zambia (n = 12). Single-genome analysis of full-length T/F Env sequences revealed that all 21 individuals were infected with a highly homogeneous population of viral variants, which were categorized as subtype C (n = 12), A1 (n = 7), or recombinant AC (n = 2). An extensive amino acid sequence-based analysis of variable loop lengths and glycosylation patterns in the T/F Envs revealed that a lower ratio of NXS to NXT-encoded glycan motifs correlated with neutralization breadth. Further analysis comparing amino acid sequence changes, insertions/deletions, and glycan motif alterations between the T/F Env and autologous early Env variants revealed that extensive diversification focused in the V2, V4, and V5 regions of gp120, accompanied by contemporaneous viral escape, significantly favored the development of breadth. These results suggest that more efficient glycosylation of subtype A and C T/F Envs through fewer NXS-encoded glycan sites is more likely to elicit antibodies that can transition from autologous to heterologous neutralizing activity following exposure to gp120

www.iavi.org), which is funded by the United States Agency for International Development and other donors listed at www.iavi.org. The funders had no role in study design, data collection and analysis, decision to publish, or preparation of the manuscript.

Competing Interests: The authors have declared that no competing interests exist.

diversification. This initiates an Env-antibody co-evolution cycle that increases neutralization breadth, and is further augmented over time by additional viral and host factors. These findings suggest that understanding how variation in the efficiency of site-specific glycosylation influences neutralizing antibody elicitation and targeting could advance the design of immunogens aimed at inducing antibodies that can transition from autologous to heterologous neutralizing activity.

Author Summary

HIV-1 has proven difficult to vaccinate against due to its ability to generate high levels of genetic diversity, particularly in the envelope glycoproteins. An ideal prophylactic vaccine would therefore elicit immune responses capable of blocking the full range of HIV-1 variants to which a population might be exposed. An essential component of protective immunity against HIV-1 is likely to be an antibody response that is capable of neutralizing genetically diverse HIV-1 viral variants. In an effort to understand how this type of 'broad' antibody response develops during natural HIV-1 infection, a large cohort study recently found that certain factors, such as high viral load, HLA-A*03 genotype, and subtype C infection, were correlated with the development of greater neutralization breadth. Here we investigated the viral envelope proteins and antibody responses in early infection in a small subset of individuals from two of the African sites included in the larger cohort study. We found that a marker for the efficiency of envelope glycosylation in the infecting viral variant was strongly correlated with the development of antibodies with greater neutralization breadth. We also found that extensive viral changes in the V2, V4, and V5 regions of the envelope gp120 protein, were strongly associated with the development of antibodies with greater neutralization breadth. Based on these results, we propose that more efficient glycosylation of the envelope protein of the infecting viral variant elicits neutralizing antibodies that drive early and complex amino acid changes in gp120, which triggers the development of antibodies whose neutralization breadth can be augmented over time by additional viral and host factors. These findings suggest that a better understanding of the efficiency of envelope glycosylation in HIV-1 could inform current vaccine strategies aimed at eliciting antibodies with neutralization breadth.

Introduction

HIV-1 has proven difficult to vaccinate against due, in part, to its ability to generate high levels of genetic diversity. During error-prone reverse transcription, up to 3.4×10^{-5} mutations per base pair can be introduced, and recombination can occur between the two viral genomes contained within a single virion [1,2]. Since HIV-1 group M emerged in the human population, these diversification mechanisms have led to the evolution of nine genetically distinct subtypes, as well as numerous circulating recombinant forms (CRFs) [3,4]. An ideal prophylactic vaccine would therefore elicit immune responses capable of blocking the full range of HIV-1 variants to which a population might be exposed, which differs based on geography.

The HIV-1 envelope (Env) glycoprotein subunits gp120 and gp41 are the targets of neutralizing antibodies, which are perhaps the most important correlate of vaccine-mediated protection against other viral diseases. HIV-1 Env gp120 exhibits the highest amount of amino acid variation throughout the entire proteome, creating a formidable obstacle for generating

neutralizing antibody-based protection [5–7]. This is exemplified by the fact that most HIV-1 infected individuals develop robust neutralizing antibodies within a few months against the infecting virus, but these antibodies are strain-specific, and lead to viral escape [8–17]. However, in a substantial fraction of infected individuals, these strain-specific antibodies evolve to acquire neutralization activity against heterologous HIV-1 Env variants over time [18–22]. To gain insight into this process, a previous study evaluated whether early Env diversity impacted neutralization breadth, which was measured at approximately 5 years post-infection in 26 HIV-1 individuals infected predominantly with subtype A [23]. In that study, diversity was measured in the Env gp120 V1-V5 region using proviral DNA-derived sequences sampled between 17 to 299 days after infection. Early Env diversity was positively associated with later development of neutralization breadth, leading the authors to propose a model in which the process of neutralization breadth begins in early infection. Indeed, others have shown that the T/F Env and/or early escape variants can trigger the development of a specific broadly neutralizing antibody lineage [15,24–26]. However, our inability to reproduce this phenomenon via vaccination reflects a significant gap in our understanding of this process.

The development of neutralization breadth during HIV-1 infection is best understood as being a complex and continuous interplay between the host immune response and the evolving viral quasispecies [15,17,24–32]. Viral replication capacity, Env diversity, super-infection, and high viral load may all contribute to the antigenic stimulation necessary to augment heterologous neutralization breadth [21,23,27,31,33–36]. Certain HIV-1 Env characteristics, often related to subtype or glycans, may also favor the development of neutralization breadth [9,19,33,36–38]. Host immunologic factors such as T follicular helper cell activity and activation within the B and T cell compartments could also modulate the development and maintenance of neutralization breadth [39–41]. MHC Class I alleles that target CD8 T cell epitopes and influence HIV-1 disease progression could also impact the development of neutralization breadth [36,42]. On the other hand, despite strong evidence that HIV-1 pathogenesis and immune activation differs between males and females [43–48], a recent study carried out by the IAVI Protocol C team of investigators was among the first to report that there was no difference in the development of neutralization between males and females [36]. In that study, 439 participants from IAVI Protocol C at nine sites across Uganda, Kenya, Rwanda, Zambia, and South Africa were evaluated for heterologous neutralization potency and breadth starting at approximately 24 months after infection. These individuals were infected predominantly with HIV-1 subtypes A1, C, and D, the proportion of which varied depending on the location of the site. The strongest correlates of neutralization breadth that emerged in the IAVI cohort study were high viral load, low CD4 T cell count, subtype C HIV-1 infection, and HLA-A*03 genotype. Thus, from a broad perspective, there are viral and host factors that create a more favorable environment for neutralization breadth to develop during natural infection. However, none of these factors can fully predict whether an individual will develop strong neutralization. We therefore investigated early viral and immune events in individuals from this same cohort to determine their role in priming the development of neutralization breadth within a natural infection setting.

In the present study, we have examined features of the T/F Envs, patterns of early Env diversification, and the autologous neutralization responses in early HIV-1 infection. Our analysis revealed that T/F Envs with fewer NXS-encoded glycan motifs, which are associated with less efficient N-linked glycosylation, were correlated with the development of greater neutralization breadth. Of note, a previous study reported that the opposite association was found in early Envs from a clade B cohort, suggesting that Env glycosylation could be a strong determinant of breadth in a clade-specific manner [38]. Neutralizing antibody-driven diversification in the Env gp120 V2, V4, and V5 regions was also a strong contributor to the development of

heterologous neutralization breadth. Thus, our finding that correlates of neutralization breadth are present in a panel of individuals in the first weeks to months after infection suggests that this process must be initiated and perpetuated during early infection by Env and antibody interactions, but is further amplified over time by a complex constellation of additional viral and host factors [36].

Results

Patient neutralizing antibody responses exhibit a wide range of breadth and potency at 3 years post infection

As the first step to understanding the development of neutralization breadth, we characterized the T/F Env variants, early longitudinal Env variants, and the autologous neutralizing antibody response in HIV-1 infected individuals from Lusaka, Zambia ($n = 12$) and Kigali, Rwanda ($n = 9$). We have reported that early autologous neutralizing antibody responses that develop in individuals in these cohorts are often potent but are invariably specific for the infecting strain [9–12]. Indeed, in the parent IAVI cohort study, heterologous neutralization was detected in less than 2% of individuals at 24 months post-infection [36]. The ability to neutralize heterologous Env variants that the immune response has not encountered, loosely defined as neutralization breadth, has been shown to develop in plasma by around 2–4 years after HIV-1 infection, in anywhere from 10 to 80% of individuals, depending on the nature of the cohort, timing of sample collection, and the methods used to evaluate and quantify breadth [18,21,22,33,34,36,41,49,50]. In agreement with these findings, neutralization scores indicative of breadth in the IAVI study were generally first observed at a mean of 3.5 years [36]. Therefore, to assess the level of neutralization breadth that developed in our smaller subset of individuals, we independently evaluated plasma samples collected at a median of 3.0 years (ranging from 1.1 to 3.5 years) after the first p24 antigen positive test (Fig 1; collectively referred to as 3-year plasma) for their capacity to neutralize a panel of 12 globally representative, tier 2 Env pseudoviruses, from a parent panel of 219 HIV-1 Env variants, as described by [51]. Numerous other studies have characterized HIV-1 plasma neutralization breadth using similar panels of 6 to 12 genetically diverse Env variants [11,36,40,50–56]. Since neutralization by the plasma samples at the lowest dilution tested (1:20) did not always achieve 50% inhibition, we calculated the Area Under the Curve (AUC) for each plasma-Env combination (21 plasma samples \times 12 Envs) for a total of 252 infectivity curves each containing a series of 5-fold dilutions. A heatmap of the neutralization AUC values is shown in S1A Fig. Neutralization IC₅₀ titers were also calculated for each plasma-Env combination, and are provided in a heatmap shown in S1B Fig. These parameters were highly correlated as expected (Spearman's $r = -0.99$, $p < 0.0001$). Using this approach, plasma samples with the most potent neutralizing activity yielded the smallest AUCs, while large AUC values were observed for poor neutralizers, thus inversely related to the IC₅₀ titer dilution. The median AUC was calculated for each individual's plasma S1A Fig and used as a continuous variable to rank neutralization breadth [51,57].

Individual plasma neutralization curves for the subjects with the highest (Z1800M) and lowest (R1135M) overall neutralization breadth against the 12 reference Envs are shown in Fig 2A and 2B. Z1800M plasma completely neutralized ten of the reference panel Envs, which included subtypes C, B, A, G, and recombinant forms CRF01_AE, CRF07_BC, and AC, with IC₅₀ titers in the 1:100 to 1:1,000 range (Fig 2A). The neutralizing activity against the two remaining Envs did not reach 100% but was substantial. This participant was also ranked as the best neutralizer out of 439 individuals tested in the larger IAVI study [36]. In contrast, plasma from subject R1135M had very limited neutralizing activity against all panel Envs, including the clade-matched subtype A reference Env, which did not reach 50% neutralization

RZHRG Coded ID	IAVI Parent Study Code	Breadth Ranking	Neut AUC	IAVI breadth score	T/F Env Subtype	Cohort site	Days since MRCA	Days since infection	Plasma breadth, years post-infection	6-month viral load	12-month viral load	HLA-A alleles	
Z1800M	PC068	1	0.6	2.33	C	ZEHRP	29	29	3.3	145000	3690	3002	3002
Z1792M	PC080	2	1.6	1.00	C	ZEHRP	14	22	3.5	40600	38200	0201	2301
Z185F	NA	3	1.7	ND	C	ZEHRP	87	33	2.2	222000	91678	3002	6802
R1141M	PC046	4	2.1	0.33	A1	PSF	26	30	3.0	13500	6440	3002	6802
Z1024F	PC048	5	2.2	1.17	C	ZEHRP	19	22	3.2	29600	51000	0205	3402
R1142F	PC049	6	2.2	0.67	A/C	PSF	16	22	3.0	51400	31500	0201	3101
Z221M	NA	7	2.3	ND	C	ZEHRP	68	22	3.0	82400	89952	0301	3101
Z1022M	PC318	8	2.5	ND	C	ZEHRP	27	55	2.1	129000	30700	0202	7401
Z1023M	NA	9	2.6	ND	C	ZEHRP	94	22	3.0	146000	144000	0301	6602
Z1781M	PC183	10	2.6	0.17	C	ZEHRP	17	22	3.4	182	13848	3001	3002
Z205F	NA	11	2.7	ND	C	ZEHRP	100	48	3.2	4330	400	3001	3601
R53F	PC005	12	3.0	0.33	A1	PSF	29	35	3.0	999	609	6802	7401
R283F	PC135	13	3.0	0.17	A1	PSF	7	22	3.0	733	4840	0205	2301
R774F	PC088	14	3.0	0.33	A1	PSF	51	65	3.0	13900	17900	0201	3601
R880F	PC085	15	3.1	0.33	A1	PSF	23	33	3.0	49	224	0201	0301
Z153M	NA	16	3.2	ND	C	ZEHRP	70	ND	2.7	unknown	unknown	3002	6802
R463F	NA	17	3.3	ND	A1	PSF	96	30	1.1	398000	76200	0101	3002
Z1047M	PC220	18	3.7	0.17	C	ZEHRP	47	33	3.2	241000	538000	3002	3301
Z201M	NA	19	3.8	ND	C	ZEHRP	74	22	2.0	204	43119	0301	3301
R66M	NA	20	3.9	ND	A/C	PSF	ND	22	3.0	750000	192000	0101	3002
R1135M	PC136	21	4.1	0.00	A1	PSF	13	26	3.4	49	49	2301	3002

Fig 1. Summary of HIV-1 infected participants. The Rwanda-Zambia HIV Research Group (RZHRG) coded identification numbers for all subjects are shown, along with the associated code assigned in [36]. Individuals are listed in the order of their breadth ranking, based on the median AUC values, when plasma was tested against a panel of 12 globally representative tier 2 Envelopes (Fig 2C). The International AIDS Vaccine Initiative (IAVI) breadth score is taken from [36]. Relevant information is shown in subsequent columns, including the subtype of the T/F Env: cohort site (Zambia-Emory HIV Research Project or ZEHRP; Projct San Francisco or PSF): days since most recent common ancestor (MRCA) calculated using the Los Alamos HIV Database tool Poisson Fitter v2 [58]; days since infection estimated using methods described by [59]; time point in years post-infection when breadth was assessed; as well as the 6- and 12-month plasma viral loads (copies per ml) and HLA-A alleles determined as described in [60]. NA indicates not applicable; ND indicates not determined.

doi:10.1371/journal.ppat.1005989.g001

(Fig 2B). R1135M was ranked at #372 out of 381 participants whose follow-up extended across 24 to 48 visit months in the IAVI study, and thus exhibited poor neutralization breadth in both studies [36]. Overall, the median AUC values for the 21 plasma samples ranged from high (AUC = 0.57) to low (AUC = 4.13) neutralization breadth (Fig 2C).

For the 12 Protocol C participants that were independently analyzed in the present study and in the larger IAVI study (i.e. had an IAVI breadth score from [36], shown in Fig 1), we compared the median AUC calculated here to the maximum breadth score (sMAX) assigned in the larger study, and found that the ranking of these individuals was highly correlated as expected (S2 Fig; Spearman's $r = -0.79$, $p = 0.002$). Median AUC values were also significantly correlated to breadth scores at Protocol C visits 36 and 42 (S2 Fig; $r = -0.76$, $p = 0.002$; $r = -0.65$, $p = 0.006$, respectively). Thus, despite using a smaller and less diverse population of HIV-1 infected subjects, a continuous variable ranking system, a different reference Env panel, and evaluation of a single time point, we detected a quantitatively similar spectrum of neutralization breadth as that reported in the IAVI study.

A lower ratio of NXS to NXT-encoded glycan motifs in the T/F Env favor the development of nAb breadth

Features of HIV-1 Env have been previously associated with the level and type of neutralization breadth that develops within an individual [9,33,38]. Indeed, in the IAVI study involving multiple HIV-1 subtypes, subtype C infection was a significant correlate of higher neutralization breadth score [36]. However, depending on the segment of the viral genome used and the timing of sample collection, subtype determination may not fully reflect the Env glycoproteins, and also may not represent the Env of the T/F virus. Here, we assigned subtypes based on the

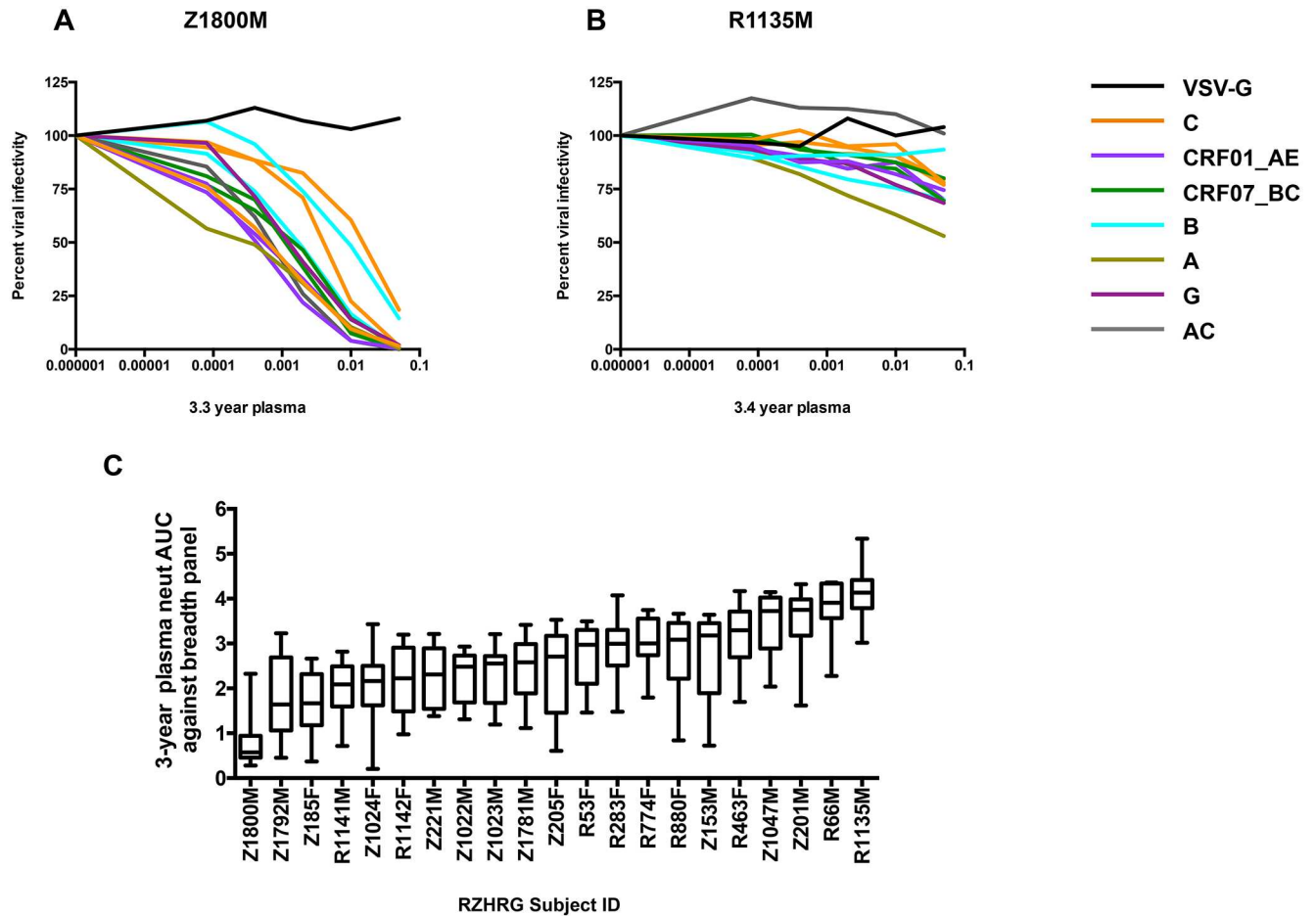


Fig 2. Evaluation of heterologous neutralization breadth in plasma samples from 21 recently HIV-1 infected individuals. Infectivity curves depicting neutralization activity against a panel of 12 global reference Env pseudoviruses described in [51] in the TZM-bl assay are shown for subjects Z1800M (A) and R1135M (B). These two subjects were chosen to demonstrate the highest and lowest level of neutralization breadth. Each curve represents neutralization of one of the 12 reference Envs, and is color coded by the subtype or circulating recombinant form (CRF) designation, as indicated in the key. Neutralization of VSV-G pseudotyped virus is shown as a negative control with a black curve. The y-axis indicates percent viral infectivity relative to 100%, which is the amount of luciferase produced in pseudovirus-infected TZM-bl cells in the absence of test plasma. The x-axis indicates the reciprocal dilution of the individual's plasma plotted on a \log_{10} scale. The Area Under the Curve (AUC) was calculated from each infectivity curve to quantify neutralization potency and breadth. The median and range for the neutralization AUC values calculated for each subject's plasma against the 12 Env reference panel are in shown in (C). High AUC values indicate weak neutralization activity, while low AUC values indicate strong neutralization activity. All AUC values are shown in S1A Fig, with the accompanying IC50 titers shown in S1B Fig.

doi:10.1371/journal.ppat.1005989.g002

full-length T/F Env sequences, which are the antigens that initiated the autologous neutralizing antibody response. We utilized plasma and/or PBMC samples collected at a median of 28 estimated days after infection (range 22 to 65 days; Fig 1) to capture the T/F Env sequences using single genome PCR amplification (SGA) [9,61–64]. We utilized the LANL Highlighter tool (https://www.hiv.lanl.gov/content/sequence/HIGHLIGHT/highlighter_top.html) and the LANL Poisson Fitter v2 tool (http://www.hiv.lanl.gov/content/sequence/POISSON_FITTER/poisson_fitter.html) to characterize the T/F Env sequences (Highlighter plots of all T/F Env sequences are shown in S3 Fig). Between 5 and 31 T/F Env sequences were analyzed for each individual, noting that fewer sequences were available for Z185F, Z221M, Z205F, Z153M, and Z201M, the subjects that were studied prior to the initiation of Protocol C. Two individuals, R53F and Z1800M, were infected with two distinguishable variants that differed systematically

at one or two polymorphisms, respectively. These observations could indicate infection by two highly similar but distinct variants from the donor quasispecies, or reflect early selection pressure on Env. Since we do not have the donor Env sequences from these individuals, we cannot distinguish between the two scenarios. Regardless, only the dominant T/F polymorphism was observed at subsequent time points for both individuals.

Overall, the analysis of T/F Env sequences suggested infection by a single variant in majority of individuals (S3 Fig). This predominance of single variant infections is consistent with our previous study of subtype A and C HIV-1 infected transmission pairs in PSF and ZEHRP, where 18 out of 20 infections were initiated by a single variant [64]. The subtype of the T/F Envs was then determined using the LANL Recombinant Identification Program (RIP) (<http://www.hiv.lanl.gov/content/sequence/RIP/RIP.html>) [65,66] or the REGA HIV-1 Automated Subtyping Tool (<http://dbpartners.stanford.edu:8080/RegaSubtyping/stanford-hiv/typingtool/>) [67]. Seven of the 9 PSF participants in Kigali were infected with an HIV-1 subtype A1 Env variant, and the remaining 2 were each infected with a unique A/C recombinant Env (S4 Fig). All 12 individuals from the ZEHRP site in Lusaka were infected with a subtype C HIV-1 Env variant. This distribution of subtypes is also consistent with our previous studies in the ZEHRP and PSF cohorts [9,62,64,68] and with the larger IAVI study [36].

A number of studies have attempted to identify amino acid signatures, glycosylation patterns, and effects of variable loop lengths in Env that are associated with the development of neutralization breadth, as this could reveal an attractive target for vaccine immunogen design [38,69,70]. To this end, we sought to identify signatures of breadth in the T/F Envs in our cohort. Amino acid signatures of neutralization breadth previously identified by others did not emerge as correlates in our cohort [38,69]. We also examined whether the length of the variable loops or the total number of N-linked glycosylation motifs correlated with neutralization breadth (Fig 3A). Interestingly, the feature that was significantly correlated with breadth in our cohort was the ratio of NXS to NXT glycosylation sites found within the gp120 region of T/F Envs (Fig 3B, S5 Fig). N-linked glycosylation motifs are generally encoded with the amino acid motifs NXS or NXT, with X indicating any amino acid except proline; however, glycosylation at NXT occurs at a higher probability than NXS that can be as much as 40% [71,72]. Interestingly, van den Kerkhof et al previously reported a connection between the NXS/total glycans ratio in early Envs and the development of breadth in a subtype B HIV-1 infected cohort [38]. However in that study, the authors observed a higher ratio of NXS to total glycosylation sites in patients who developed breadth, postulating that a lower probability of Env gp120 glycosylation could favor breadth. We observed a contrasting effect in our mixed subtype, non-B cohort (Fig 3). While the total number of glycosylation sites in gp120 did not correlate with breadth, the ratio of NXS to NXT sites was correlated with neutralization breadth AUC ($r = 0.56$, $p = 0.008$). That is, individuals infected with T/F Env variants encoding fewer NXS glycan motifs ($r = 0.50$, $p = 0.02$) and more NXT sites ($r = -0.45$, $p = 0.04$) in gp120, and by extension a higher probability of glycosylation, were more likely to develop greater breadth. The discrepancy between van der Kerkhof et al and our study could reflect differences in the cohorts, experimental methods, Env sampling times, or time frame when neutralization breadth was measured. Furthermore, numerous biological distinctions have been reported in Env glycosylation, antigenicity, and immunogenicity, as well as in transmission and disease progression, based on HIV-1 subtype [6,9,36,46,64,68,73–80]. Indeed striking differences in conservation and variability of glycosylation sites are seen within and between HIV-1 subtypes [76,81,82]. Even the presence of relatively 'conserved' glycosylation positions can vary from less than 25% to over 90%, depending on subtype [76]. It is therefore not surprising that the efficiency of early Env glycosylation could impact the development of neutralization breadth in a clade-specific manner.

A

	Variable	r	p value
Median AUC vs.	V1 length	-0.19	0.42
	V2 length	-0.13	0.57
	V1+V2 length	-0.17	0.47
	V3 length	0.37	0.10
	V4 length	0.12	0.61
	V5 length	-0.31	0.17
	gp120 glycan #	-0.16	0.48
	gp120 NXS #	0.50	0.02
	gp120 NXT #	-0.45	0.04
gp120 NXS:NXT	0.56	0.008	

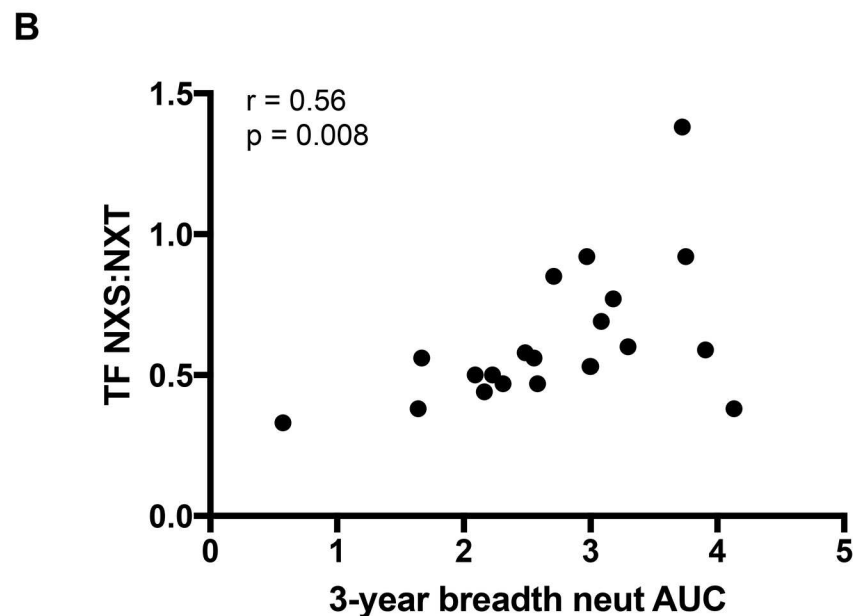


Fig 3. Correlation of T/F Env features with neutralization breadth. T/F Env amino acid sequence features for 21 subjects were defined using the LANL N-GlycoSite and Variable Region Characteristics online tools. A) Spearman’s correlations were performed between neutralization breadth AUC and variable loop lengths, number of total, (NXS + NXT), NXS, and NXT glycan motifs (excluding X = proline) in gp120, and the ratio of NXS motifs divided by NXT motifs. Spearman’s r values and p values are shown for each comparison. P values < 0.05 are considered significant. B) Scatter plot of median 3-year breadth AUC value vs ratio of NXS: NXT sites in the transmitted/founder Env. Spearman correlation $r = 0.56$, $p = 0.008$.

doi:10.1371/journal.ppat.1005989.g003

Complex early Env diversification in hyper-variable regions contributes to neutralization breadth

We next sought to gain insight into whether early Env diversification influenced subsequent neutralization breadth in our cohort of subjects. To understand the shifts from the T/F Env to a more diverse quasispecies due to selective pressures, we analyzed SGA derived full-length ‘early’ Env sequences derived from plasma and/or PBMC samples collected after the development of potent strain-specific neutralizing antibodies [9,11,12]. Because nucleotide-based

dN/dS analyses are problematic when resampling the same population over short periods of time [83], and do not fully reflect the range of diversity that occurs within Env at the amino acid level (conservative vs. non-conservative amino acid changes, insertions and deletions, alterations to glycosylation sites), we developed and implemented a novel approach for statistically quantifying early Env diversity. First, FASTA amino acid alignments of the T/F Envs and early Envs from the same patient were subjected to Sequence Harmony analysis to identify amino acid positions that were significantly different between the two groups of sequences (Z -score ≤ -3) [38,63,84]. As a proof of concept for this approach, we first analyzed sequences from subject R880F, whose early neutralizing antibody responses and escape pathways had been previously mapped in our laboratory in great detail [11]. Sequence Harmony analysis not only confirmed our previous findings of neutralizing antibody escape mechanisms at 3-months and 6-months after infection (Fig 4A and 4B, respectively), which were characterized through extensive Env mutagenesis and neutralization assays, but also identified an additional four positions where the amino acid composition at 6-months post-infection had significantly shifted from the T/F Envs (Fig 4B). Sequence Harmony analysis was therefore performed on Env sequences from 12 subjects who had sufficient numbers of Env sequences available (minimum of 15 total sequences) from an early longitudinal plasma sample, which ranged from 3.7 to 7.7 months after infection.

Next, to take into account the biochemical nature of the identified changes in amino acid composition, we developed an Immunotype Diversity Index (IDI) that reflected the complexity of diversification that occurred in Env, particularly in highly variable regions. This approach is based on the premise that antibodies must be exposed to variation within their epitopes, i.e. immunotypes, to acquire heterologous neutralization breadth [19,27]. The IDI score was calculated as follows: For amino acid positions with Z -scores < -3 , a conservative amino acid change was given 0.5 points; while a non-conservative change, an insertion or deletion, and a purifying selection event were each given 1 point. It is important to note, that this approach takes into account all SGA derived T/F Env sequences, as opposed to using a consensus T/F Env as a point of comparison. This analysis can therefore factor in the presence of amino acid diversity near the time of infection, thus allows for the identification of purifying events. Multiple amino acid changes at a single position (e.g. in R880F, position 338 shifts from E in the T/F Env to G, A, D, or K in the 6-month Env population, Fig 4B) were given appropriate points for each possible change (0.5 or 1, depending on the nature of the change), and added together. Furthermore, if the amino acid change resulted in an introduction, deletion, or shift of a glycosylation site, the significant position was given an additional point. For example, in R880F at position 335 (Fig 4A), there was a non-conservative change from S to N (1 point) that shifted a glycosylation motif (1 point), giving amino acid position 335 a total of 2 points. The final value for each identified position was multiplied by the absolute value of the calculated Z -score, to factor in the statistical significance of the change. That is, a non-conservative amino acid change that just meets the significance threshold (-3) will have 3 points, but is not weighted equally to the same change with a highly significant Z -score of -30 , which will result in 30 points.

The final IDI score was calculated for each patient by taking the sum of all points for all significant positions (Fig 5). Overall, the IDI scores varied over almost 10-fold, ranging from 263 in Z1800M to 28 in R66M, demonstrating broad variation in the amount of early Env diversity in our cohort (Fig 5). S6A Fig shows an amino acid alignment for Z1800M, with regions that factored into the IDI score highlighted, as a representative example of high Env diversity that is concentrated in V2, V4, and V5. The same is shown for R66M in S6B Fig to represent low Env diversity. When the IDI scores for full-length T/F Env were plotted against median AUC neutralization breadth scores, there was a significant negative correlation (Spearman's $r = -0.60$, $p = 0.04$; Fig 6A). Thus, complex and dramatic amino acid changes associated with stronger

A R880F 3-month Envs

Amino Acid Position	Score	Z-score	Group 1 (n=33)	Group 2 (n=10)
141	1	nan	N	N
283	1	nan	V	V
292	1	nan	Q	Q
*295	0.83	-4.19	I	Itr
*335	1	nan	S	S
*338	0.6	-7.27	E	DKEg
*341	0.95	-1.78	D	Dn
*456	0.76	-6.57	E	KE
820	1	nan	D	D
825	0.89	-4.45	A	At

B R880F 6-month Envs

Amino Acid Position	Score	Z-score	Group 1 (n=33)	Group 2 (n=12)
141	0.81	-5.92	N	SN
283	0.86	-5.11	V	Va
292	0.91	-3.14	Q	Qk
*295	0.91	-2.97	I	Ir
*335	0.86	-4.13	S	Sn
*338	0.35	-11.94	E	Gadek
*341	0.75	-7.21	D	ND
*456	0.75	-6.94	E	KE
820	0.69	-7.66	D	NDe
825	1	nan	A	A

Fig 4. Validation of the Immunotype Diversity Index approach to quantify Env diversification using R880F. Subject R880F was chosen to validate the Sequence Harmony approach because the earliest neutralizing antibody response was previously mapped to an epitope located at the base of the V3 loop [11]. Positions indicated with an asterisk were identified and evaluated in the previous study. Thirty-three SGA derived T/F Env amino acid sequences from R880F (Group 1) were aligned with 10 sequences from 3-months post-infection (A), or 12 sequences from 6-months post-infection (B) (Group 2). In (A), Sequence Harmony analysis identified four positions, highlighted yellow, that were significantly different ($Z < -3$) between the two populations at 3-months. Two of these positions were determined to be autologous neutralizing antibody escape mutations at 3-months via mutagenesis (295 and 338), whereas 456 could not be directly attributed to neutralizing antibody or cytotoxic T lymphocyte selective pressure. In (B), Sequence Harmony analysis identified two positions that remained significant from 3 months (highlighted yellow), six positions that became significant at 6 months (highlighted green), and two positions that lost significance at 6 months (not highlighted). Positions 335, 338, and 341 were all determined to be neutralizing antibody escape mutations at 6 months.

doi:10.1371/journal.ppat.1005989.g004

selection in Env were correlated with greater breadth. However, much of the significant Env amino acid diversity was occurring in the V2, V4, and V5 regions of Env gp120 (see S6A Fig for an example). When IDI scores were calculated using only these three regions, a much stronger correlation was observed (Spearman's $r = -0.80$, $p = 0.003$; Fig 6B). Thus, complex changes

Subject	Immunotype Diversity Index (IDI)	V2-V4-V5 IDI	# T/F Env sequences	# 4-8 month Env sequences
Z1800M	263	232	13	12
Z185F	96	36	10	9
R1141M	59	27	24	7
Z1024F	102	30	13	9
R1142F	66	7	26	13
Z1022M	161	61	20	8
Z1023M	118	54	12	12
R53F	73	18	20	10
R774F	27	4	12	8
R880F	88	7	34	12
Z153M	54	0	10	5
R66M	28	0	15	6

Fig 5. Immunotype Diversity Index scores for 12 subjects. For each position where Z-scores were less than -3 in Sequence Harmony analysis, the nature of the change, in addition to shifts in glycans and the significance of the difference, was taken into account when calculating the Immunotype Diversity Index. Changes (conservative = 0.5; non-conservative, deletions, purifying selection = 1, glycan shift or deletion = 1) were multiplied by absolute value of Z-scores to factor in significance, and added together for a final IDI. These values ranged from 28 to 263. When IDI was restricted to significant positions within V2, V4, and V5, the values ranged from 0 to 232. The number of T/F Env sequences and longitudinal Env sequences from 4–8 months included in this analysis are indicated.

doi:10.1371/journal.ppat.1005989.g005

in V2, V4, and V5 of gp120 appear to play a particularly strong role in driving the development of neutralization breadth in our cohort.

Early Env diversity is linked with selective pressure exerted by autologous neutralizing antibodies

Sequence diversity within Env during early HIV-1 infection is likely to be the result of pressure exerted predominantly by replicative capacity, cytotoxic T-cell responses, and autologous neutralizing antibodies [10–12,85–87]. For 11 of the 21 individuals, we had sufficient samples available to directly evaluate autologous neutralization against the T/F Env and contemporaneous Envs at an early time point ranging from 2 to 12 months (median of 5 months). As autologous neutralizing antibody responses are generally more potent than heterologous responses, we calculated the neutralization IC50 titers for the T/F Env and contemporaneous Envs for these 11 individuals. If we were unable to calculate the IC50 titer due to lack of neutralization activity, we used a value of 20. The autologous neutralization IC50 titers for the T/F Envs ranged from 32 to 2,580, while the titers for neutralization of the contemporaneous Envs were lower, ranging from 20 to 267 (Figs 7 and 8). As a group, the T/F Envs were significantly more sensitive to neutralization by the early autologous plasma than were the contemporaneous Envs, indicating that escape from autologous neutralizing antibodies had occurred during this time period (Fig 7, Wilcoxon matched-pairs signed rank test, $p = 0.002$). The magnitude of escape was then quantified by dividing the T/F IC50 titer by the contemporaneous titer. The magnitude of escape ranged from 1 (i.e. Z201M), meaning there was essentially no difference

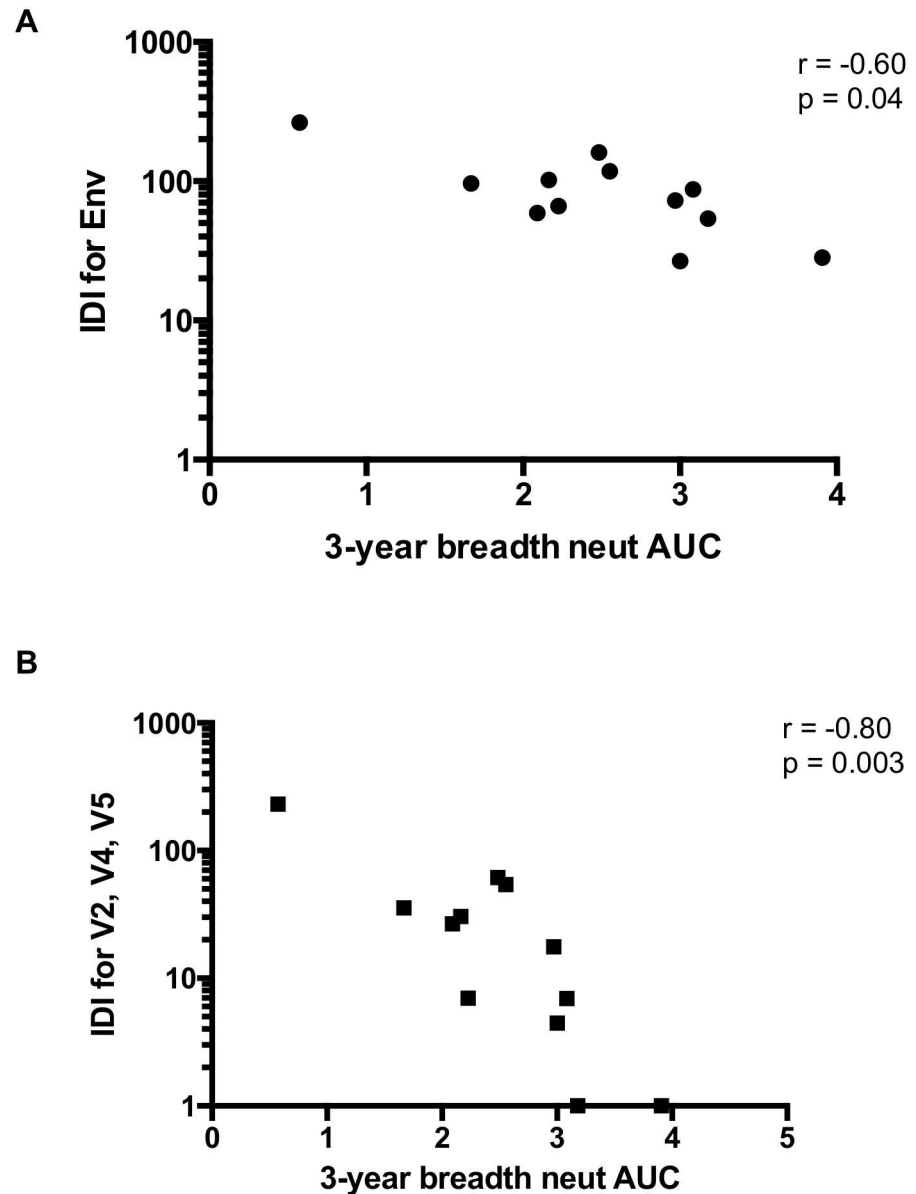


Fig 6. Correlation of Immunity Diversity Index scores with neutralization breadth. **A)** Spearman's correlation of IDI scores with median AUC breadth scores ($n = 12$) revealed a relationship between early Env diversity and later development of neutralization breadth ($r = -0.60$, $p = 0.04$). **B)** This correlation was stronger when IDI scores only included diversity found within the V2, V4, and V5 variable loops ($r = -0.80$, $p = 0.003$). Two patients with V2-V4-V5 scores of zero were given a value of 1 for illustrative purposes on the log10 scale.

doi:10.1371/journal.ppat.1005989.g006

between neutralization susceptibility of the T/F Env and the contemporaneous Envs, to 112 (Z185F) (Fig 8). We also evaluated the ability of the 3-year 'late' plasma (that was used to determine breadth) to neutralize the T/F Env, and these IC50 titers ranged from 850 to 25,342. We next performed a non-parametric Spearman's correlation analysis using these variables, along with the ratio of NXS:NXT sites in the T/F Env and the 12-month viral load, to examine potential relationships between these factors and the development of neutralization breadth.

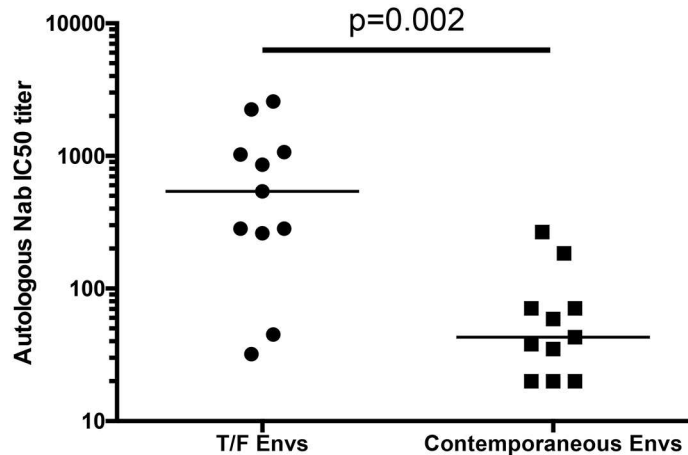


Fig 7. Autologous early neutralization of T/F Envs vs. contemporaneous Envs. For 11 patients, sampling allowed neutralization assays to be performed on T/F Envs, and Envs from an early time-point (range 2 to 12 months, median 5 months), with the early time-point plasma listed in Fig 8. Wilcoxon matched-pairs signed rank test revealed a significant difference between neutralization IC50 titer of the early plasma vs. T/F Envs, compared to the same plasma against the contemporaneous Envs ($p = 0.002$).

doi:10.1371/journal.ppat.1005989.g007

As expected, the neutralization IC50 and AUC values against the global reference panel were strongly inversely correlated (Fig 9; Spearman’s $r = -0.99$, $p < 0.0001$). Interestingly, even within this smaller subset of subjects, the ratio of NXS to NXT glycan motifs in the T/F Env gp120 proteins was again significantly correlated with the development of neutralization breadth using either measurement (Fig 9; Spearman’s $r = -0.82$, $p = 0.003$ for IC50; $r = 0.80$, $p = 0.005$ for AUC). The NXS:NXT ratio was also strongly and inversely correlated with the magnitude of escape (Spearman’s $r = -0.83$, $p = 0.002$). Thus, potentially higher efficiency of glycosylation in gp120 was associated with a higher magnitude of early escape from autologous neutralizing antibodies and the development of neutralization breadth. The potency of T/F Env neutralization was also correlated directly and significantly with the magnitude of escape (Spearman’s $r = 0.76$, $p = 0.008$), underscoring the importance of a dynamic relationship between the T/F Env, early neutralizing antibodies, and viral escape. The importance of this

Subject ID	NXS:NXT	Early T/F IC50	Time point	Cont IC50	Escape	IDI	V2-V4-V5 IDI	12-month VL	Late T/F IC50	Global Panel IC50	Global Panel AUC
Z1800M	0.33	540	5	20	27	263	232	3690	3605	1030	0.6
Z185F	0.56	2238	5	20	112	96	36	91678	7758	205	1.7
R1141M	0.50	261	5	38	7	59	27	6440	8019	168	2.1
Z221M	0.47	1026	5	59	17	ND	ND	89952	1452	79	2.3
Z1022M	0.58	2580	3	35	74	161	61	30700	25342	71	2.5
Z205F	0.85	860	2	267	3	ND	ND	400	9010	44	2.7
R53F	0.92	45	6	20	2	73	18	609	1145	29	3
R880F	0.69	283	3	71	4	88	7	224	14977	23	3.1
Z153M	0.77	1070	12	184	6	54	0	750000	1022	21	3.2
R463F	0.60	283	3	71	4	ND	ND	76200	14219	22	3.3
Z201M	0.92	32	8	43	1	ND	ND	43119	850	20	3.8

Fig 8. Summary of quantitative factors that potentially contribute to neutralization breadth. Autologous plasma neutralization IC50 titers for the T/F Env and contemporaneous Envs from an early time point ranging from 2 to 12 months (median 5 months) is shown for 11 patients, along with the ratio of NXS to NXT glycan sites in the T/F gp120, the magnitude of escape (T/F Env IC50 divided by contemporaneous Env IC50), full Env and V2-V4-V5 IDI values, and the 12-month plasma viral load. The neutralization IC50 titer of 3-year plasma against the autologous T/F Env and the heterologous global reference Env panel is shown, in addition to the neutralization AUC against the global reference panel.

doi:10.1371/journal.ppat.1005989.g008

A

Spearman's Rho

Variable	T/F IC50	Cont IC50	Escape	Late T/F IC50	IDI	V2-V4-V5 IDI	12-month VL	Panel IC50	Panel AUC
Ratio NXS to NXT	-0.41	0.35	-0.83	-0.27	-0.54	-0.75	-0.19	-0.82	0.80
T/F IC50		0.04	0.76	0.31	0.43	0.36	0.43	0.37	-0.41
Cont IC50			-0.42	0.13	-0.63	-0.70	0.00	-0.58	0.57
Escape				0.31	0.57	0.71	0.39	0.75	-0.77
Late T/F IC50					0.43	0.36	-0.39	0.24	-0.17
IDI						0.86	-0.21	0.68	-0.68
V2-V4-V5 score							0.00	0.89	-0.89
12-month VL								-0.08	0.05
Panel IC50									-0.99

B

p value

Variable	T/F IC50	Cont IC50	Escape	Late T/F IC50	IDI	V2-V4-V5 IDI	12-month VL	Panel IC50	Panel AUC
Ratio NXS to NXT	0.205	0.283	0.002	0.418	0.236	0.066	0.577	0.003	0.005
T/F IC50		0.905	0.008	0.344	0.354	0.444	0.184	0.263	0.210
Cont IC50			0.198	0.695	0.152	0.105	0.995	0.064	0.071
Escape				0.344	0.200	0.088	0.239	0.010	0.008
Late T/F IC50					0.354	0.444	0.237	0.485	0.615
IDI						0.024	0.662	0.110	0.110
V2-V4-V5 score							1.037	0.012	0.012
12-month VL								0.818	0.881
Panel IC50									<.0001

Fig 9. Spearman's correlation analysis of quantitative factors and neutralization breadth. **A)** Spearman's rho values are shown for each pairwise correlation analysis between variables. **B)** p-values are shown for each pairwise correlation analysis between variables. A p value < 0.05 was considered significant.

doi:10.1371/journal.ppat.1005989.g009

early co-evolutionary process is further substantiated by the fact that both the V2-V4-V5 IDI and the magnitude of escape were also strongly correlated with the development of greater breadth (V2-V4-V5 IDI: Spearman's $r = 0.89$, $p = 0.012$ for IC50; $r = -0.89$, $p = 0.012$ for AUC; Escape: Spearman's $r = 0.75$, $p = 0.010$ for IC50; $r = -0.77$, $p = 0.008$ for AUC).

Discussion

A major goal for HIV-1 vaccine development is to induce neutralizing antibodies that are capable of broadly protecting against a globally diverse population of viral variants. To this end, various studies have attempted to identify signatures within HIV-1 Env or clinical/host factors that correlate with the development of breadth [10,21,22,31,36,38,69,77,88], on the basis that they could be targeted by immunization strategies. We postulated that factors present as early as several weeks after infection could also be determinants for subsequent development of breadth, as early Env diversity was previously linked with breadth [23]. Using a panel of individuals exhibiting a spectrum of neutralization breadth that was highly correlated with that found for the larger parent cohort [36], we analyzed the inter-dependent relationships between the T/F Env; Env diversification, neutralizing antibodies, and viral escape during the first months of infection; and development of neutralization breadth several years later. Our focus on early infection stems partly from the observation that generic correlates (i.e. high viral load,

subtype C infection) cannot fully explain the development of breadth, as there are many individuals that have these characteristics but fail to develop broad heterologous neutralization capacity. In addition, understanding which early viral and immune events are associated with generating desirable antibody responses during infection could most directly inform strategies to transition from vaccine-induced strain-specific autologous neutralizing antibodies, which have been recently elicited by trimer-based immunogens [89,90], to those with broader neutralizing capacity.

Our observations suggest that the long process of developing neutralization breadth is initiated at least in part by glycosylation of the T/F Env, and is perpetuated by antibody-driven Env diversification in gp120 hyper-variable regions. Our findings are also consistent with previous reports that tracked broadening of a neutralizing antibody lineage within single individuals [24,26,27]. However, further augmentation by factors linked to viral load or disease progression may also be necessary to develop high levels of neutralization breadth, but are more difficult to translate into immunization strategies [36]. Currently, it is unknown how parameters such as viral subtype and HLA-A alleles could contribute to the broadening of the neutralizing antibody response. One possible explanation is that subtype C HIV-1 infection generates higher plasma viral loads than subtype A infection [46]. Furthermore, HLA alleles can influence the immune response to HIV-1 infection and disease progression via both innate and adaptive immune pathways in the same cohort, and thus could have durable or transient effects that act at different stages of infection [46].

Regarding the impact of the T/F Env, our finding that fewer NXS glycan motifs favor the development of neutralization breadth highlights the important and incompletely understood relationship between Env glycosylation and immunogenicity. Various models of glycan site occupancy have revealed a strong preference for glycosylation at NXT over NXS [71,72,91–94]. This could result from NXT providing a more optimal conformation of the acceptor sequence, with increased nucleophilicity of the asparagine amide group [91]. Furthermore, kinetics studies have demonstrated that the eukaryotic oligosaccharyltransferase enzyme has a higher affinity for NXT sites compared to NXS [95,96]. NXT motifs are also positively selected for in adjacent sequons, and are more likely than NXS to be glycosylated in this setting [97]. Other factors, such as the flanking sequences, tertiary protein structure, and proximity to the C-terminus of the protein, as well as the amino acid at the X position, could also influence the probability and extent of glycosylation at individual sites, but have not systematically been investigated [98,99].

Although glycosylation is a common protein modification, lentiviral proteins are particularly heavily glycosylated [100], with carbohydrate moieties accounting for about 50% of the mass of HIV-1 Env [101,102]. Remarkable variation in the number and position of glycan motifs across variants has long been recognized as a defining feature of HIV-1 Env [76,81,82], and evasion from neutralizing antibodies has been proposed as a major function of this 'glycan shield' [8]. In the context of the Env trimer, an extensive glycan 'canopy' consists of around 90 N-linked carbohydrate moieties that exist in crowded and dispersed configurations, are under-processed compared to host glycans, and form inter-dependent clusters [103,104]. The oligomeric nature and dense packing of glycans of HIV-1 Env restricts its glycan processing in the golgi such that most glycans are oligomannose, but micro-heterogeneity in carbohydrate forms is observed at individual glycan addition sites [103–106]. The glycan array is known to have a strong influence on Env structure and antigenicity, as well as modulating antibody recognition. Indeed, removal of a single glycan site can influence neutralizing antibody recognition at distal locations as well as reducing the overall oligomannose content by more than predicted [104]. Glycosylation of gp120 could also influence the mucosal transmissibility of HIV-1, depending on the clade and cohort examined [64,68,78,79,107,108]. Our findings, combined with those

from previous studies, suggest that the use of NXS vs. NXT in HIV-1 Env could be an additional means for the virus to modulate its structure, immunogenicity, and sensitivity to neutralizing antibodies [10,38]. Recovery and characterization of numerous bnAbs from chronically infected individuals has demonstrated that many of these antibodies have the capacity to target glycans directly [56,109–122]. Even bnAbs that do not target glycans directly, such as VRC01, have acquired unique adaptations that allow the antibody to avoid glycan clashes and tolerate Env diversity [123–125]. Further underscoring the importance of Env glycosylation to vaccine development, Env SOSIP trimer immunogens based on clade B JR-FL and clade A BG505 Envs elicited tier 2 neutralizing antibodies, but their activity was restricted at least in part by the fact that the neutralizing antibodies that targeted glycan ‘holes’, where a particular glycan motif is absent [89,90]. Although we did not find that the absence or presence of a specific glycan(s) was associated with the development of breadth in our cohort, it is possible that T/F Envs with fewer NXS sites are less likely to have glycan ‘holes’, and preferentially elicit antibodies with a greater capacity to acquire breadth in response to Env diversification. Thus, as stated by [126], glycans have ‘enormous relevance’ to HIV-1 vaccine design. It is therefore notable that a potential marker for efficiency of Env glycosylation has emerged in this study, and in a distinct study by [38], as an early clade-specific signal that may contribute to the development of neutralization breadth.

Currently, a substantial effort is being devoted to designing and testing novel HIV-1 Env immunogens that preserve features of the native trimer and/or are derived from patients who developed broadly neutralizing antibody activity [89,127–133]. These Env immunogens could be readily varied in terms of glycosylation and immunotype diversity, and assessed experimentally, whereas it is less clear how to incorporate sustained viral replication, continuing Env diversity, genotypic host features, and other correlates of breadth via a vaccination protocol. Our results are encouraging for vaccine design because they suggest that modulating Env glycosylation in a clade-specific manner could produce immunogens that are even better suited to elicit neutralizing antibodies with the potential to transition to heterologous breadth. Then, if one can develop immunotype mimics based on diversification of the hyper-variable domains, antibody lineages may be able to develop tolerance for diversity and glycans, and acquire heterologous neutralizing activity to relevant targets. On the other hand, Env diversity presented in the absence of the neutralizing antibody response that provided the selective pressure may be unable to fully recapitulate the evolution of bnAb in immunized animal models [134,135]. However, the strategic selection and presentation of the priming Env appears to be of vital importance, as we have shown for SIV vaccination in nonhuman primate studies [136].

It is important to consider that, during HIV-1 infection, neutralizing antibodies tend to have limited specificities, including the CD4 binding site, V1V2, and the base of the V3 loop, that differ between individuals [10–12,15–17,27,137]. It is unclear why some individuals, such as R66M studied here, produce antibodies with limited neutralizing capacity against the autologous T/F Env while others, such as Z1800M, produce potent neutralizing antibodies within the same time frame. It is possible that, in addition to differences in subtype, the higher NXS to NXT ratio of the R66M T/F Env compared to the Z1800M T/F Env could also have initiated this disparity. Our findings highlight a void in our understanding of the importance of the immunogenicity and antigenicity of the T/F Env, and the early anti-Env antibody landscape, in terms of germline activation, clonality, and binding affinity, on the ability to transition from strain-specific to heterologous neutralization. Broadly neutralizing antibody lineages, such as VRC01 or CAP256, do not develop in isolation; they stem from autologous neutralizing antibodies in an environment that includes competition and influence by a milieu of other B cells and antibodies, occurring in the presence of ongoing viral diversity [27,138]. Current studies have begun to bridge the gap between strain-specific and broadly neutralizing antibodies by focusing on the longitudinal

evolution of an individual bnAb lineage [24–27,138]. Others have developed strategies to design Env antigens that engage specific B-cell germline lineages with known potential to evolve into a broadly neutralizing antibody [139,140]. However, even this strategically designed Env immunogen engaged other germlines, in addition to the germline of interest, suggesting that the complexity of the human immune system will be a formidable obstacle to reproducing the activation and maturation of individual bnAb lineages [139]. Taken together, our observations provide new insight into the importance of T/F Env glycosylation, autologous neutralizing antibodies, diversification in gp120, and viral escape in setting the course to neutralization breadth. With the successful elicitation of tier 2 autologous neutralizing antibodies using trimer-based immunogens [89,90], additional promising Env immunogens on the horizon, and a more complete understanding of glycosylation in the context of several genetically diverse Env trimers [103,104], it may be possible to optimize the glycosylation of these reagents so that they preferentially elicit neutralizing antibodies with the potential to acquire heterologous neutralizing capacity. Whether necessary cycles of antibody-virus co-evolution, and other factors, can then be reproduced in the absence of infection to augment this process will remain to be determined.

Materials and Methods

Ethics statement

The ZEHRP, PSF, and IAVI Protocol C participants were selected based on rapid screening of adults with recent history of HIV exposure in Rwanda and Zambia. After obtaining written informed consent, blood samples were collected from HIV-1 infected participants longitudinally. The procedures for written informed consent and research activities were approved by institutional review boards at all collaborating clinical research centers, with further compliance to human experimentation guidelines set forth by the United States Department of Health and Human Services. The study was reviewed and approved by the Republic of Rwanda National Ethics Committee, Emory University Institutional Review Board, and the University of Zambia Research Ethics Committee.

Study population

The 21 HIV-1 infected individuals studied were identified shortly after a transmission event through their enrollment in two HIV-discordant couple cohorts (see Fig 1). Zambian participants were from the Zambia-Emory HIV Research Project (ZEHRP, established in 1994 by Dr. Susan Allen) in Lusaka and the Rwandan participants were from Projet San Francisco (PSF, established in 1986 by Dr. Susan Allen) in Kigali. Together, these two sites accounted for roughly 43% of participants in the larger IAVI study [36]. These projects were originally designed as ‘couples voluntary counseling and testing’ clinics and have been described previously [64,141]. ZEHRP and PSF are also part of the Rwanda Zambia HIV Research Group at Emory University (RZHRG; <http://www.rzhr.org>). More recently Protocol C, a uniform vaccine-preparedness study developed and implemented by the International AIDS Vaccine Initiative (IAVI; <http://www.iavi.org>), was initiated and carried out at multiple sites in Africa, including ZEHRP and PSF [80].

The 21 individuals studied here were selected prior to the initiation of the larger IAVI study. The subjects were chosen based on three factors: a p24 antigen positive test (i.e. infection detected in the early Fiebig stages); the availability of early longitudinal plasma samples; and for Protocol C participants, the availability of viable PBMC collected during early infection (for studies that are not included in these analyses). Z185F, Z221M, Z205E, Z153M, and Z201M were enrolled in ZEHRP prior to Protocol C. The remaining 16 subjects were enrolled in Protocol C at the time of sampling. Twelve of 16 the Protocol C participants were analyzed in both

the present study and in the larger IAVI study (see Fig 1; note that while there are 13 Parent Study participants with PC codes listed in the second column, Z1022M/PC138 was not analyzed in the larger study and thus has no breadth score in the fifth column) [36].

The procedures for written informed consent and research activities were approved by institutional review boards at all collaborating clinical research centers, with further compliance to human experimentation guidelines set forth by the United States Department of Health and Human Services. Plasma viral load determinations were underwritten by IAVI and performed at Contract Lab Services (CLS) in South Africa using an Abbott m2000 system. The typical range of detection was between 160 and 4×10^7 RNA copies/ml. HLA genotyping was performed using a combination of PCR-based techniques as described previously [60,142].

PCR amplification and cloning of HIV-1 *env* genes

For 16 of 21 individuals, cDNA synthesis and 384-well single genome PCR amplification (SGA) was performed essentially as described in [61] S3 Fig. Briefly, RNA was extracted from cryopreserved patient plasma samples using the QIAmp viral RNA, and reverse transcription was performed using the SuperScript III kit (Invitrogen) with reverse primer OFM19 (5'-GCACTCAAGGCAAGCTTTATTGAGGCTTA-3'). cDNA was diluted to result in <30% positive wells for SGA. First round PCR was performed in a 15 μ L volume using the Phusion Hot-start II High Fidelity DNA Polymerase (Thermo Scientific) with forward primer Vif1 (5'-GGGTTTATTACAGGGACAGCA GAG-3') and OFM19. Cycling conditions were 98°C for 2 min; 10 cycles of 95°C for 15 s, 54°C for 60 s, and 68°C for 4 min; 25 cycles of 95°C for 15 s, 54°C for 60 s, and 68°C for 4 min, adding 5 s to the extension per cycle; 72°C for 30 min; and 4°C hold. Second round PCR was performed with the same enzyme in a 10 μ L volume with 1 μ L of the first round of PCR and EnvA-TOPO (5'-CACCGCCTTAGGCATCTCCTATGG CAGGAAGAA-3') and EnvN (5'-CTGTCAATCAGGGAAGTAGCCTTGTGT-3'). Cycling conditions were 95°C for 2 min; 30 cycles of 95°C for 15 s, 54°C for 60 s, and 72°C for 2.5 min; 72°C for 10 min; and 4°C hold. PCR amplicons were purified using Qiagen PCR Clean-Up Kit. For Z201M, Z205F, Z221M, Z185F, and Z153M, full-length *env* genes were amplified previously using 96-well SGA from plasma and PBMC, as described [9]. PCR amplified *env* genes plus flanking sequences were T/A-cloned into one of several pCR3.1-based expression vectors as described [9,11,61].

Sequence analyses of HIV-1 *env* genes

On average, 13 SGA PCR amplicons per patient (range 5 to 31) per time-point were sequenced with Beckman Coulter Genomics using the following primers: For13 (5'-GAGAAAGAGCA GAAGACAGTGG-3'); For15 (5'-CAGCACAGTA CAATGTACACATGGAA-3'); For17 (5'-AGCAGCAGGAAGCACTATGGGCG C-3'); For19 (5'-GGAACCTGTGCCTCTTCAGC TACC-3'); and Rev14 (5'-ACCATGTTATTTTCCACATGTTAAA-3'); Rev16 (5'-ATGG GAGGGGCATACATTGCT-3'); Rev17 (5'-CCTGGAGCTGTTAATGCCCCAGAC-3'); and Rev19 (5'-ACTTTTGGACCACTTGCCACCCAT-3'). Sequencher v5 was used to generate nucleotide sequence contigs, and sequences with evidence of mixed peaks were omitted from the analysis. Additionally, previously reported sequences were utilized for patients Z205F, Z185F, Z201M, Z221M, Z153M, and R880F [9–12,143,144]. Geneious v6.1.7 was used to align and translate nucleotide sequences. Amino acid alignments were exported from Geneious in FASTA format and used to generate Highlighter plots (http://www.hiv.lanl.gov/content/sequence/HIGHLIGHT/highlighter_top.html), to define Env features (<http://www.hiv.lanl.gov/content/sequence/GLYCOSITE/glycosite.html>) and (http://www.hiv.lanl.gov/content/sequence/VAR_REG_CHAR/index.html), and perform Sequence Harmony comparisons

(<http://www.ibi.vu.nl/programs/shmrwww/>). Subtype reference Env nucleotide sequences were obtained from the Los Alamos Sequence Database (<http://www.hiv.lanl.gov/content/sequence/NEWALIGN/align.html>). A Neighbor-joining nucleotide phylogenetic tree was generated in Geneious v6.1.7. HIV-1 subtyping was performed with REGA HIV-1 Automated Subtyping Tool (<http://dbpartners.stanford.edu:8080/RegaSubtyping/stanford-hiv/typingtool/>) [67]. The days since the most common recent ancestor (MRCA) are presented in Fig 1, and were determined by analyzing the T/F Env sequences for each subject in the Poisson Fitter v2 tool from the Los Alamos HIV Database (http://www.hiv.lanl.gov/content/sequence/POISSON_FITTER/pfitter.html) [58,145]. The estimated days since infection values, also presented in Fig 1, were calculated using the methods of [59]. The T/F *env* nucleotide sequences have been submitted under Genbank accession numbers KX983471-KX983929.

For calculation of IDI scores, Sequence Harmony comparisons were used to identify amino acid positions significantly different between the T/F and 4–8 month sequences (Z-score < -3). For significant positions, points were given as follows: 0.5 points: conservative changes; 1 point: non-conservative changes, deletions, insertions, purifying selection; 1 point: shift, deletion, or insertion of glycosylation motif. Multiple changes at significant positions were given cumulative points. Sum of points at significant positions were multiplied by the absolute value of the Z-score at corresponding position to weight scores by statistical significance. Final IDI for each patient was calculated by adding all points for all positions. For V2-V4-V5 scores, significant positions were restricted to these locations, as identified by LANL HIV Variable Region Characterization tool.

Neutralization assay

A global panel of 12 HIV-1 Env reference clones developed by deCamp *et al.* was obtained through the NIH AIDS Reagent Program (Catalog number 12670) [51]. Generation of Env pseudoviruses and performing the TZM-bl neutralization assay has been described previously [9–12,40,61,68,136,144,146–150]. Briefly, Env-expressing plasmids were co-transfected with the HIV-1 SG3ΔEnv proviral backbone into 293T cells using Fugene HD (Promega), and pseudovirus stocks were collected 48h post-transfection, clarified by centrifugation, and frozen at -80°C. In all cases except one, plasma was used to evaluate heterologous and autologous neutralization. Because R66M began antiretroviral therapy approximately 1.25 years post-infection, IgG antibodies were purified from 36-month plasma using a GE Healthcare Life Sciences Ab SpinTrap, according to manufacturer instructions (GE 28-4083-47). The concentration of the purified IgG was determined by ELISA, and was used in place of plasma in neutralization assays. Five-fold serial dilutions of heat-inactivated plasma samples or purified IgG were assayed for their inhibitory potential against the Env pseudoviruses using the TZM-bl indicator cell line, with luciferase as the readout. At 48 hours post-infection, cells were lysed and luciferase activity was measured using a BioTek Cytation 3 imaging reader with Gen5 v2.07 Software. The average background luminescence from a series of uninfected wells was subtracted from each experimental well. Assays were run in duplicate and repeated independently at least twice.

Statistical analyses

All graphs were generated in Prism v6.0. Virus infectivity curves were generated and Area Under the Curve was calculated in Prism and used for comparisons of neutralization activity. Neutralization IC₅₀ titers were also calculated in Prism from the virus infectivity curve using log transformation of x-values, normalization of y-values, and linear regression of dose-response inhibition with variable slope. A Mann-Whitney test or Wilcoxon matched pairs analysis was used to compare two groups, while a Kruskal-Wallis test was used for to compare

more than two groups. A non-parametric Spearman's test was used to assess correlations between variables in Prism v6.0. P values less than 0.05 were considered to be significant.

Supporting Information

S1 Fig. Neutralization Area Under the Curve (AUC) and IC50 titers heat maps for plasma from 21 HIV-1 infected individuals against the 12 Env global reference panel. Five-fold serial dilutions of plasma samples from each individual (RZHRG coded IDs are shown; see Fig 1) were assayed for neutralization against a panel of globally representative tier 2 Env pseudoviruses, as well as a VSV-G pseudotyped negative control. **A)** The AUC was calculated from each infectivity curve and color-coded on a continuous relative scale from the lowest AUC value (0.3, green) to highest (6.3, red) to visualize differences in breadth and potency of neutralization. **B)** The neutralization 50% inhibition (IC50) titer was calculated from each infectivity curve and color-coded on a continuous relative scale from the lowest IC50 titer (20 indicating that an IC50 could not be calculated, green) to the highest IC50 titer (7424, red) to visualize differences in breadth and potency of neutralization. Note that on both heat maps green indicates the most potent neutralization, while red indicates the least potent.

(TIF)

S2 Fig. Neutralization breadth ranking was highly correlated with that determined in the larger IAVI study. For 12 individuals that were analyzed by [36] and in the present study, a Spearman Rank correlation test was performed using the maximum breadth score (sMAX, based on plasma from multiple time points) and the neutralization breadth AUC determine here using plasma from approximately 3-years post infection. The rankings were highly inversely correlated ($r = -0.79$, $p = 0.002$), indicating that high sMAX scores corresponded to low breadth AUC values. The sMAX values were plotted on the y-axis against the neutralization breadth AUC on the x-axis. IAVI breadth scores at 36 (red) and 42 (blue) months were also significantly correlated with neutralization breadth AUC.

(TIF)

S3 Fig. Highlighter plots of T/F Env sequences. (A-E) Single genome PCR amplification (SGA) derived full-length *env* sequences were isolated from 21 patients near the time of infection (median 28 estimated days after infection, range 22 to 65 days). Translated amino acid sequences were aligned, and the LANL Highlighter tool was used to illustrate sequence variation using ticks colored as indicated in the legend.

(PDF)

S4 Fig. Phylogenetic tree and recombination breakpoints. A selection of 15 Subtype Reference Sequences was downloaded from the LANL sequence database and were aligned with the consensus of each set of patient derived T/F Env sequences. The resulting neighbor-joining phylogenetic tree, shown in (A), illustrates Zambian derived Envs clustering with the Subtype C reference sequences, while the majority of Rwandan sequences cluster with Subtype A1. The exceptions to this, R1142F (B) and R66M (C), were analyzed via the REGA HIV-1 Subtyping Tool to identify contributing components of these recombinant Envs.

(TIF)

S5 Fig. NXS and NXT glycan motifs within T/F Env gp120 sequences. (A) An amino acid alignment of 21 T/F Env gp120 sequences was analyzed for glycosylation sequon and position using LANL N-GlycoSite (<https://www.hiv.lanl.gov/content/sequence/GLYCOSITE/glycosite.html>). Numbering includes amino acid position according to the T/F Env alignment, and

relative to HXB2 in parentheses. Variable regions are highlighted above the position numbers. The number of NXS, NXT, and total glycans, and NXS:NXT ratio is included for each sequence. **(B)** To determine if NXS:NXT ratios were driven by differences in a specific region of Env, data was divided into the top 10 neutralizers (#1–10) and bottom 11 neutralizers (#11–21) based on breadth ranking. NXS:NXT ratios were calculated for V1, V2, C2, V3, C3, V4, C4, and V5 regions of gp120 by dividing the number of NXS sites in that region by the number of NXT sites for each group of T/F Envs. The T/F Envs from the bottom 11 neutralizers had higher NXS:NXT ratios in V1, V2, C2, C3, V4, and C4, highlighted in yellow, but not in V3 and V5.

(TIF)

S6 Fig. Amino acid alignments of Env for Z1800M and R66M. Env amino acid alignments are shown for Z1800M (A) and R66M (B), including sequences from the first time point after infection (estimated to be 29 days for Z1800M and 22 days for R66M, Fig 1) and the longitudinal time point used to calculate the Immunity Diversity Index score (5-months for Z1800M and R66M). The Env IDI scores for Z1800M and R66M were 263 and 28, respectively (Fig 5). The V2, V4, V5 IDI scores were 232 and 0, respectively (Fig 5). The sequences from the 5-month time point are shaded gray. Yellow highlighting indicates positions that were identified by Sequence Harmony as having a Z-score less than -3. gp120 variable domains are indicated above the sequences.

(PDF)

Acknowledgments

This study was made possible through samples and data collected as part of the Zambia-Emory HIV Research Project (ZEHRP), Project San Francisco (PSF), the Zambia Rwanda HIV Research Group (ZRHRG) at Emory University, and the International AIDS Vaccine Initiative (IAVI) Protocol C Research Network. We gratefully acknowledge the staff, interns, and participants of the Zambian and Rwandan cohorts. We thank Dr. James Tang for HLA typing data, Dr. Ling Yue and Dr. Jesus Salazar-Gonzalez for providing *env* sequences, and Bing Li, Lori Spicer, and Katie Kilgore for technical support. We thank Dr. Tianwei Yu and Dr. Robert Lyles of the Emory CFAR Biostatistical and Bioinformatics Core for discussions about statistical analysis. The contents of this manuscript are the responsibility of the authors and do not necessarily reflect the views of USAID or the United States Government. The panel of 12 global HIV-1 Env Clones (cat# 12670) was obtained through the NIH AIDS Reagent Program, Division of AIDS, NIAID, NIH from Dr. David Montefiori [51].

Author Contributions

Conceptualization: CAD SAS.

Formal analysis: CAD SAS SLB.

Funding acquisition: CAD.

Investigation: SAS SLB.

Methodology: CAD SAS.

Project administration: CAD.

Resources: WK SL EK MP SA EH.

Supervision: CAD.

Writing – original draft: CAD SAS.

Writing – review & editing: CAD SAS WK SL EK MP SA EH.

References

1. Mansky LM, Temin HM (1995) Lower in vivo mutation rate of human immunodeficiency virus type 1 than that predicted from the fidelity of purified reverse transcriptase. *J Virol* 69: 5087–5094. PMID: [7541846](#)
2. Jetzt AE, Yu H, Klarmann GJ, Ron Y, Preston BD, et al. (2000) High rate of recombination throughout the human immunodeficiency virus type 1 genome. *J Virol* 74: 1234–1240. PMID: [10627533](#)
3. Robertson DL, Anderson JP, Bradac JA, Carr JK, Foley B, et al. (2000) HIV-1 nomenclature proposal. *Science* 288: 55–56. PMID: [10766634](#)
4. Worobey M, Gemmel M, Teuwen DE, Haselkorn T, Kunstman K, et al. (2008) Direct evidence of extensive diversity of HIV-1 in Kinshasa by 1960. *Nature* 455: 661–664. doi: [10.1038/nature07390](#) PMID: [18833279](#)
5. Starcich BR, Hahn BH, Shaw GM, McNeely PD, Modrow S, et al. (1986) Identification and characterization of conserved and variable regions in the envelope gene of HTLV-III/LAV, the retrovirus of AIDS. *Cell* 45: 637–648. PMID: [2423250](#)
6. Gaschen B, Taylor J, Yusim K, Foley B, Gao F, et al. (2002) Diversity considerations in HIV-1 vaccine selection. *Science* 296: 2354–2360. doi: [10.1126/science.1070441](#) PMID: [12089434](#)
7. Taylor BS, Sobieszczyk ME, McCutchan FE, Hammer SM (2008) The challenge of HIV-1 subtype diversity. *N Engl J Med* 358: 1590–1602. doi: [10.1056/NEJMra0706737](#) PMID: [18403767](#)
8. Wei X, Decker J.M., Wang S., Hui H., Kappes J.C., Wu X., Salazar J.F., Salazar M.G., Kilby J.M., Saag M.S., Komarova N.L., Nowak M.A., Hahn B.H., Kwong P.D., Shaw G.M. (2003) Antibody Neutralization and Escape by HIV-1. *Nature* 422: 307–312. doi: [10.1038/nature01470](#) PMID: [12646921](#)
9. Li B, Decker JM, Johnson RW, Bibollet-Ruche F, Wei X, et al. (2006) Evidence for potent autologous neutralizing antibody titers and compact envelopes in early infection with subtype C human immunodeficiency virus type 1. *J Virol* 80: 5211–5218. doi: [10.1128/JVI.00201-06](#) PMID: [16699001](#)
10. Lynch RM, Rong R, Boliar S, Sethi A, Li B, et al. (2011) The B cell response is redundant and highly focused on V1V2 during early subtype C infection in a Zambian seroconverter. *J Virol* 85: 905–915. doi: [10.1128/JVI.02006-10](#) PMID: [20980495](#)
11. Murphy MK, Yue L, Pan R, Boliar S, Sethi A, et al. (2013) Viral escape from neutralizing antibodies in early subtype A HIV-1 infection drives an increase in autologous neutralization breadth. *PLoS Pathog* 9: e1003173. doi: [10.1371/journal.ppat.1003173](#) PMID: [23468623](#)
12. Rong R, Li B, Lynch RM, Haaland RE, Murphy MK, et al. (2009) Escape from autologous neutralizing antibodies in acute/early subtype C HIV-1 infection requires multiple pathways. *PLoS Pathog* 5: e1000594. doi: [10.1371/journal.ppat.1000594](#) PMID: [19763269](#)
13. Gray ES, Moore PL, Choge IA, Decker JM, Bibollet-Ruche F, et al. (2007) Neutralizing antibody responses in acute human immunodeficiency virus type 1 subtype C infection. *J Virol* 81: 6187–6196. doi: [10.1128/JVI.00239-07](#) PMID: [17409164](#)
14. Moore PL, Gray ES, Choge IA, Ranchobe N, Misana K, et al. (2008) The c3-v4 region is a major target of autologous neutralizing antibodies in human immunodeficiency virus type 1 subtype C infection. *J Virol* 82: 1860–1869. doi: [10.1128/JVI.02187-07](#) PMID: [18057243](#)
15. Moore PL, Gray ES, Wibmer CK, Bhiman JN, Nonyane M, et al. (2012) Evolution of an HIV glycan-dependent broadly neutralizing antibody epitope through immune escape. *Nat Med* 18: 1688–1692. doi: [10.1038/nm.2985](#) PMID: [23086475](#)
16. Moore PL, Ranchobe N, Lambson BE, Gray ES, Cave E, et al. (2009) Limited neutralizing antibody specificities drive neutralization escape in early HIV-1 subtype C infection. *PLoS Pathog* 5: e1000598. doi: [10.1371/journal.ppat.1000598](#) PMID: [19763271](#)
17. Wibmer CK, Bhiman JN, Gray ES, Tumba N, Abdool Karim SS, et al. (2013) Viral escape from HIV-1 neutralizing antibodies drives increased plasma neutralization breadth through sequential recognition of multiple epitopes and immunotypes. *PLoS Pathog* 9: e1003738. doi: [10.1371/journal.ppat.1003738](#) PMID: [24204277](#)
18. Hraber P, Seaman MS, Bailer RT, Mascola JR, Montefiori DC, et al. (2014) Prevalence of broadly neutralizing antibody responses during chronic HIV-1 infection. *AIDS* 28: 163–169. doi: [10.1097/QAD.000000000000106](#) PMID: [24361678](#)
19. Moore PL, Williamson C, Morris L (2015) Virological features associated with the development of broadly neutralizing antibodies to HIV-1. *Trends Microbiol.*

20. Derdeyn CA, Moore PL, Morris L (2014) Development of broadly neutralizing antibodies from autologous neutralizing antibody responses in HIV infection. *Curr Opin HIV AIDS* 9: 210–216. doi: [10.1097/COH.0000000000000057](https://doi.org/10.1097/COH.0000000000000057) PMID: [24662931](https://pubmed.ncbi.nlm.nih.gov/24662931/)
21. Gray ES, Madiga MC, Hermanus T, Moore PL, Wibmer CK, et al. (2011) The neutralization breadth of HIV-1 develops incrementally over four years and is associated with CD4+ T cell decline and high viral load during acute infection. *J Virol* 85: 4828–4840. doi: [10.1128/JVI.00198-11](https://doi.org/10.1128/JVI.00198-11) PMID: [21389135](https://pubmed.ncbi.nlm.nih.gov/21389135/)
22. Euler Z, van Gils MJ, Bunnik EM, Phung P, Schweighardt B, et al. (2010) Cross-reactive neutralizing humoral immunity does not protect from HIV type 1 disease progression. *J Infect Dis* 201: 1045–1053. doi: [10.1086/651144](https://doi.org/10.1086/651144) PMID: [20170371](https://pubmed.ncbi.nlm.nih.gov/20170371/)
23. Piantadosi A, Panteleeff D, Blish CA, Baeten JM, Jaoko W, et al. (2009) Breadth of neutralizing antibody response to human immunodeficiency virus type 1 is affected by factors early in infection but does not influence disease progression. *J Virol* 83: 10269–10274. doi: [10.1128/JVI.01149-09](https://doi.org/10.1128/JVI.01149-09) PMID: [19640996](https://pubmed.ncbi.nlm.nih.gov/19640996/)
24. Liao HX, Lynch R, Zhou T, Gao F, Alam SM, et al. (2013) Co-evolution of a broadly neutralizing HIV-1 antibody and founder virus. *Nature* 496: 469–476. doi: [10.1038/nature12053](https://doi.org/10.1038/nature12053) PMID: [23552890](https://pubmed.ncbi.nlm.nih.gov/23552890/)
25. Bonsignori M, Zhou T, Sheng Z, Chen L, Gao F, et al. (2016) Maturation Pathway from Germline to Broad HIV-1 Neutralizer of a CD4-Mimic Antibody. *Cell* 165: 449–463. doi: [10.1016/j.cell.2016.02.022](https://doi.org/10.1016/j.cell.2016.02.022) PMID: [26949186](https://pubmed.ncbi.nlm.nih.gov/26949186/)
26. Doria-Rose NA, Schramm CA, Gorman J, Moore PL, Bhiman JN, et al. (2014) Developmental pathway for potent V1V2-directed HIV-neutralizing antibodies. *Nature* 509: 55–62. doi: [10.1038/nature13036](https://doi.org/10.1038/nature13036) PMID: [24590074](https://pubmed.ncbi.nlm.nih.gov/24590074/)
27. Bhiman JN, Anthony C, Doria-Rose NA, Karimanzira O, Schramm CA, et al. (2015) Viral variants that initiate and drive maturation of V1V2-directed HIV-1 broadly neutralizing antibodies. *Nat Med*.
28. Bosch KA, Rainwater S, Jaoko W, Overbaugh J (2009) Temporal analysis of HIV envelope sequence evolution and antibody escape in a subtype A-infected individual with a broad neutralizing antibody response. *Virology* 398: 115–124.
29. Moore PL, Sheward D, Nonyane M, Ranchobe N, Hermanus T, et al. (2013) Multiple pathways of escape from HIV broadly cross-neutralizing V2-dependent antibodies. *J Virol*.
30. Moore PL, Gray ES, Sheward D, Madiga M, Ranchobe N, et al. (2011) Potent and broad neutralization of HIV-1 subtype C by plasma antibodies targeting a quaternary epitope including residues in the V2 loop. *J Virol* 85: 3128–3141. doi: [10.1128/JVI.02658-10](https://doi.org/10.1128/JVI.02658-10) PMID: [21270156](https://pubmed.ncbi.nlm.nih.gov/21270156/)
31. Sather DN, Armann J, Ching LK, Mavrantoni A, Sellhorn G, et al. (2009) Factors associated with the development of cross-reactive neutralizing antibodies during human immunodeficiency virus type 1 infection. *J Virol* 83: 757–769. doi: [10.1128/JVI.02036-08](https://doi.org/10.1128/JVI.02036-08) PMID: [18987148](https://pubmed.ncbi.nlm.nih.gov/18987148/)
32. Sather DN, Carbonetti S, Malherbe DC, Pissani F, Stuart AB, et al. (2014) Emergence of broadly neutralizing antibodies and viral coevolution in two subjects during the early stages of infection with human immunodeficiency virus type 1. *J Virol* 88: 12968–12981. doi: [10.1128/JVI.01816-14](https://doi.org/10.1128/JVI.01816-14) PMID: [25122781](https://pubmed.ncbi.nlm.nih.gov/25122781/)
33. Bandawe GP, Moore PL, Werner L, Gray ES, Sheward DJ, et al. (2015) Differences in HIV type 1 neutralization breadth in 2 geographically distinct cohorts in Africa. *J Infect Dis* 211: 1461–1466. doi: [10.1093/infdis/jiu633](https://doi.org/10.1093/infdis/jiu633) PMID: [25398460](https://pubmed.ncbi.nlm.nih.gov/25398460/)
34. van Gils MJ, Euler Z, Schweighardt B, Wrin T, Schuitemaker H (2009) Prevalence of cross-reactive HIV-1-neutralizing activity in HIV-1-infected patients with rapid or slow disease progression. *AIDS* 23: 2405–2414. doi: [10.1097/QAD.0b013e32833243e7](https://doi.org/10.1097/QAD.0b013e32833243e7) PMID: [19770692](https://pubmed.ncbi.nlm.nih.gov/19770692/)
35. Cortez V, Odem-Davis K, McClelland RS, Jaoko W, Overbaugh J (2012) HIV-1 superinfection in women broadens and strengthens the neutralizing antibody response. *PLoS Pathog* 8: e1002611. doi: [10.1371/journal.ppat.1002611](https://doi.org/10.1371/journal.ppat.1002611) PMID: [22479183](https://pubmed.ncbi.nlm.nih.gov/22479183/)
36. Landais E, Huang X, Havenar-Daughton C, Murrell B, Price MA, et al. (2016) Broadly Neutralizing Antibody Responses in a Large Longitudinal Sub-Saharan HIV Primary Infection Cohort. *PLoS Pathog* 12: e1005369. doi: [10.1371/journal.ppat.1005369](https://doi.org/10.1371/journal.ppat.1005369) PMID: [26766578](https://pubmed.ncbi.nlm.nih.gov/26766578/)
37. Dreja H, O'Sullivan E, Pade C, Greene KM, Gao H, et al. (2010) Neutralization activity in a geographically diverse East London cohort of human immunodeficiency virus type 1-infected patients: clade C infection results in a stronger and broader humoral immune response than clade B infection. *J Gen Virol* 91: 2794–2803. doi: [10.1099/vir.0.024224-0](https://doi.org/10.1099/vir.0.024224-0) PMID: [20685933](https://pubmed.ncbi.nlm.nih.gov/20685933/)
38. van den Kerkhof TL, Feenstra KA, Euler Z, van Gils MJ, Rijdsdijk LW, et al. (2013) HIV-1 envelope glycoprotein signatures that correlate with the development of cross-reactive neutralizing activity. *Retrovirology* 10: 102. doi: [10.1186/1742-4690-10-102](https://doi.org/10.1186/1742-4690-10-102) PMID: [24059682](https://pubmed.ncbi.nlm.nih.gov/24059682/)
39. Locci M, Havenar-Daughton C, Landais E, Wu J, Kroenke MA, et al. (2013) Human circulating PD-(+)1CXCR3(-)CXCR5(+) memory Tfh cells are highly functional and correlate with broadly neutralizing

- HIV antibody responses. *Immunity* 39: 758–769. doi: [10.1016/j.immuni.2013.08.031](https://doi.org/10.1016/j.immuni.2013.08.031) PMID: [24035365](https://pubmed.ncbi.nlm.nih.gov/24035365/)
40. Boliar S, Murphy MK, Tran TC, Carnathan DG, Armstrong WS, et al. (2012) B-Lymphocyte Dysfunction in Chronic HIV-1 Infection Does Not Prevent Cross-Clade Neutralization Breadth. *J Virol* 86: 8031–8040. doi: [10.1128/JVI.00771-12](https://doi.org/10.1128/JVI.00771-12) PMID: [22623771](https://pubmed.ncbi.nlm.nih.gov/22623771/)
 41. Mikell I, Sather DN, Kalams SA, Altfeld M, Alter G, et al. (2011) Characteristics of the earliest cross-neutralizing antibody response to HIV-1. *PLoS Pathog* 7: e1001251. doi: [10.1371/journal.ppat.1001251](https://doi.org/10.1371/journal.ppat.1001251) PMID: [21249232](https://pubmed.ncbi.nlm.nih.gov/21249232/)
 42. Martin MP, Carrington M (2013) Immunogenetics of HIV disease. *Immunol Rev* 254: 245–264. doi: [10.1111/imr.12071](https://doi.org/10.1111/imr.12071) PMID: [23772624](https://pubmed.ncbi.nlm.nih.gov/23772624/)
 43. Fideli US, Allen SA, Musonda R, Trask S, Hahn BH, et al. (2001) Virologic and immunologic determinants of heterosexual transmission of human immunodeficiency virus type 1 in africa. *AIDS Res Hum Retroviruses* 17: 901–910. doi: [10.1089/088922201750290023](https://doi.org/10.1089/088922201750290023) PMID: [11461676](https://pubmed.ncbi.nlm.nih.gov/11461676/)
 44. Addo MM, Altfeld M (2014) Sex-based differences in HIV type 1 pathogenesis. *J Infect Dis* 209 Suppl 3: S86–92.
 45. Yue L, Prentice HA, Farmer P, Song W, He D, et al. (2013) Cumulative impact of host and viral factors on HIV-1 viral-load control during early infection. *J Virol* 87: 708–715. doi: [10.1128/JVI.02118-12](https://doi.org/10.1128/JVI.02118-12) PMID: [23115285](https://pubmed.ncbi.nlm.nih.gov/23115285/)
 46. Prentice HA, Price MA, Porter TR, Cormier E, Mugavero MJ, et al. (2014) Dynamics of viremia in primary HIV-1 infection in Africans: insights from analyses of host and viral correlates. *Virology* 449: 254–262. doi: [10.1016/j.virol.2013.11.024](https://doi.org/10.1016/j.virol.2013.11.024) PMID: [24418560](https://pubmed.ncbi.nlm.nih.gov/24418560/)
 47. Klein SL, Jedlicka A, Pekosz A (2010) The Xs and Y of immune responses to viral vaccines. *Lancet Infect Dis* 10: 338–349. doi: [10.1016/S1473-3099\(10\)70049-9](https://doi.org/10.1016/S1473-3099(10)70049-9) PMID: [20417416](https://pubmed.ncbi.nlm.nih.gov/20417416/)
 48. Klein SL, Poland GA (2013) Personalized vaccinology: one size and dose might not fit both sexes. *Vaccine* 31: 2599–2600. doi: [10.1016/j.vaccine.2013.02.070](https://doi.org/10.1016/j.vaccine.2013.02.070) PMID: [23579257](https://pubmed.ncbi.nlm.nih.gov/23579257/)
 49. Doria-Rose NA, Klein RM, Manion MM, O'Dell S, Phogat A, et al. (2009) Frequency and phenotype of human immunodeficiency virus envelope-specific B cells from patients with broadly cross-neutralizing antibodies. *J Virol* 83: 188–199. doi: [10.1128/JVI.01583-08](https://doi.org/10.1128/JVI.01583-08) PMID: [18922865](https://pubmed.ncbi.nlm.nih.gov/18922865/)
 50. Simek MD, Rida W, Priddy FH, Pung P, Carrow E, et al. (2009) Human immunodeficiency virus type 1 elite neutralizers: individuals with broad and potent neutralizing activity identified by using a high-throughput neutralization assay together with an analytical selection algorithm. *J Virol* 83: 7337–7348. doi: [10.1128/JVI.00110-09](https://doi.org/10.1128/JVI.00110-09) PMID: [19439467](https://pubmed.ncbi.nlm.nih.gov/19439467/)
 51. deCamp A, Hraber P, Bailer RT, Seaman MS, Ochsenbauer C, et al. (2014) Global panel of HIV-1 Env reference strains for standardized assessments of vaccine-elicited neutralizing antibodies. *J Virol* 88: 2489–2507. doi: [10.1128/JVI.02853-13](https://doi.org/10.1128/JVI.02853-13) PMID: [24352443](https://pubmed.ncbi.nlm.nih.gov/24352443/)
 52. Mascola JR, D'Souza P, Gilbert P, Hahn BH, Haigwood NL, et al. (2005) Recommendations for the design and use of standard virus panels to assess neutralizing antibody responses elicited by candidate human immunodeficiency virus type 1 vaccines. *J Virol* 79: 10103–10107. doi: [10.1128/JVI.79.16.10103-10107.2005](https://doi.org/10.1128/JVI.79.16.10103-10107.2005) PMID: [16051803](https://pubmed.ncbi.nlm.nih.gov/16051803/)
 53. Li M, Gao F, Mascola JR, Stamatatos L, Polonis VR, et al. (2005) Human immunodeficiency virus type 1 env clones from acute and early subtype B infections for standardized assessments of vaccine-elicited neutralizing antibodies. *J Virol* 79: 10108–10125. doi: [10.1128/JVI.79.16.10108-10125.2005](https://doi.org/10.1128/JVI.79.16.10108-10125.2005) PMID: [16051804](https://pubmed.ncbi.nlm.nih.gov/16051804/)
 54. Li M, Salazar-Gonzalez JF, Derdeyn CA, Morris L, Williamson C, et al. (2006) Genetic and neutralization properties of subtype C human immunodeficiency virus type 1 molecular env clones from acute and early heterosexually acquired infections in Southern Africa. *J Virol* 80: 11776–11790. doi: [10.1128/JVI.01730-06](https://doi.org/10.1128/JVI.01730-06) PMID: [16971434](https://pubmed.ncbi.nlm.nih.gov/16971434/)
 55. Walker LM, Simek MD, Priddy F, Gach JS, Wagner D, et al. (2010) A limited number of antibody specificities mediate broad and potent serum neutralization in selected HIV-1 infected individuals. *PLoS Pathog* 6: e1001028. doi: [10.1371/journal.ppat.1001028](https://doi.org/10.1371/journal.ppat.1001028) PMID: [20700449](https://pubmed.ncbi.nlm.nih.gov/20700449/)
 56. Walker LM, Huber M, Doores KJ, Falkowska E, Pejchal R, et al. (2011) Broad neutralization coverage of HIV by multiple highly potent antibodies. *Nature* 477: 466–470. doi: [10.1038/nature10373](https://doi.org/10.1038/nature10373) PMID: [21849977](https://pubmed.ncbi.nlm.nih.gov/21849977/)
 57. Yu X, Gilbert PB, Hioe CE, Zolla-Pazner S, Self SG (2012) Statistical approaches to analyzing HIV-1 neutralizing antibody assay data. *Stat Biopharm Res* 4: 1–13. doi: [10.1080/19466315.2011.633860](https://doi.org/10.1080/19466315.2011.633860) PMID: [24660049](https://pubmed.ncbi.nlm.nih.gov/24660049/)
 58. Giorgi EE, Funkhouser B, Athreya G, Perelson AS, Korber BT, et al. (2010) Estimating time since infection in early homogeneous HIV-1 samples using a poisson model. *BMC Bioinformatics* 11: 532. doi: [10.1186/1471-2105-11-532](https://doi.org/10.1186/1471-2105-11-532) PMID: [20973976](https://pubmed.ncbi.nlm.nih.gov/20973976/)

59. Cohen MS, Gay CL, Busch MP, Hecht FM (2010) The detection of acute HIV infection. *J Infect Dis* 202 Suppl 2: S270–277.
60. Tang J, Shao W, Yoo YJ, Brill I, Mulenga J, et al. (2008) Human leukocyte antigen class I genotypes in relation to heterosexual HIV type 1 transmission within discordant couples. *J Immunol* 181: 2626–2635. PMID: [18684953](#)
61. Burton SL, Kilgore KM, Smith SA, Reddy S, Hunter E, et al. (2015) Breakthrough of SIV strain smE660 challenge in SIV strain mac239-vaccinated rhesus macaques despite potent autologous neutralizing antibody responses. *Proc Natl Acad Sci U S A* 112: 10780–10785. doi: [10.1073/pnas.1509731112](#) PMID: [26261312](#)
62. Boeras DI, Hraber PT, Hurlston M, Evans-Strickfaden T, Bhattacharya T, et al. (2011) Role of donor genital tract HIV-1 diversity in the transmission bottleneck. *Proc Natl Acad Sci U S A* 108: E1156–1163. doi: [10.1073/pnas.1103764108](#) PMID: [22065783](#)
63. Smith SA, Kilgore KM, Kasturi SP, Pulendran B, Hunter E, et al. (2016) Signatures in Simian Immunodeficiency Virus SIVsmE660 Envelope gp120 Are Associated with Mucosal Transmission but Not Vaccination Breakthrough in Rhesus Macaques. *J Virol* 90: 1880–1887.
64. Haaland RE, Hawkins PA, Salazar-Gonzalez J, Johnson A, Tichacek A, et al. (2009) Inflammatory genital infections mitigate a severe genetic bottleneck in heterosexual transmission of subtype A and C HIV-1. *PLoS Pathog* 5: e1000274. doi: [10.1371/journal.ppat.1000274](#) PMID: [19165325](#)
65. de Oliveira T, Deforche K, Cassol S, Salminen M, Paraskevis D, et al. (2005) An automated genotyping system for analysis of HIV-1 and other microbial sequences. *Bioinformatics* 21: 3797–3800. doi: [10.1093/bioinformatics/bti607](#) PMID: [16076886](#)
66. Alcantara LC, Cassol S, Libin P, Deforche K, Pybus OG, et al. (2009) A standardized framework for accurate, high-throughput genotyping of recombinant and non-recombinant viral sequences. *Nucleic Acids Res* 37: W634–642. doi: [10.1093/nar/gkp455](#) PMID: [19483099](#)
67. Pineda-Pena AC, Faria NR, Imbrechts S, Libin P, Abecasis AB, et al. (2013) Automated subtyping of HIV-1 genetic sequences for clinical and surveillance purposes: performance evaluation of the new REGA version 3 and seven other tools. *Infect Genet Evol* 19: 337–348. doi: [10.1016/j.meegid.2013.04.032](#) PMID: [23660484](#)
68. Derdeyn CA, Decker JM, Bibollet-Ruche F, Mokili JL, Muldoon M, et al. (2004) Envelope-Constrained Neutralization-Sensitive HIV-1 After Heterosexual Transmission. *Science* 303: 2019–2022. doi: [10.1126/science.1093137](#) PMID: [15044802](#)
69. Rademeyer C, Moore PL, Taylor N, Martin DP, Choge IA, et al. (2007) Genetic characteristics of HIV-1 subtype C envelopes inducing cross-neutralizing antibodies. *Virology* 368: 172–181. doi: [10.1016/j.virol.2007.06.013](#) PMID: [17632196](#)
70. Gnanakaran S, Daniels MG, Bhattacharya T, Lapedes AS, Sethi A, et al. (2010) Genetic signatures in the envelope glycoproteins of HIV-1 that associate with broadly neutralizing antibodies. *PLoS Comput Biol* 6: e1000955. doi: [10.1371/journal.pcbi.1000955](#) PMID: [20949103](#)
71. Kasturi L, Eshleman JR, Wunner WH, Shakin-Eshleman SH (1995) The hydroxy amino acid in an Asn-X-Ser/Thr sequon can influence N-linked core glycosylation efficiency and the level of expression of a cell surface glycoprotein. *J Biol Chem* 270: 14756–14761. PMID: [7782341](#)
72. Schwarz F, Aebi M (2011) Mechanisms and principles of N-linked protein glycosylation. *Curr Opin Struct Biol* 21: 576–582. doi: [10.1016/j.sbi.2011.08.005](#) PMID: [21978957](#)
73. Gnanakaran S, Lang D, Daniels M, Bhattacharya T, Derdeyn CA, et al. (2007) Clade-specific Differences in HIV-1: Diversity and Correlations in C3-V4 Regions of gp120. *J Virol* 81: 4886–4891. doi: [10.1128/JVI.01954-06](#) PMID: [17166900](#)
74. Lynch RM, Shen T, Gnanakaran S, Derdeyn CA (2009) Appreciating HIV type 1 diversity: subtype differences in Env. *AIDS Res Hum Retroviruses* 25: 237–248. doi: [10.1089/aid.2008.0219](#) PMID: [19327047](#)
75. Sethi A, Tian J, Derdeyn CA, Korber B, Gnanakaran S (2013) A mechanistic understanding of allosteric immune escape pathways in the HIV-1 envelope glycoprotein. *PLoS Comput Biol* 9: e1003046. doi: [10.1371/journal.pcbi.1003046](#) PMID: [23696718](#)
76. Travers SA (2012) Conservation, Compensation, and Evolution of N-Linked Glycans in the HIV-1 Group M Subtypes and Circulating Recombinant Forms. *ISRN AIDS* 2012: 823605. doi: [10.5402/2012/823605](#) PMID: [24052884](#)
77. Rusert P, Kouyos RD, Kadelka C, Ebner H, Schanz M, et al. (2016) Determinants of HIV-1 broadly neutralizing antibody induction. *Nat Med*.
78. Chohan B, Lang D, Sagar M, Korber B, Lavreys L, et al. (2005) Selection for human immunodeficiency virus type 1 envelope glycosylation variants with shorter V1-V2 loop sequences occurs during

- transmission of certain genetic subtypes and may impact viral RNA levels. *J Virol* 79: 6528–6531. doi: [10.1128/JVI.79.10.6528-6531.2005](https://doi.org/10.1128/JVI.79.10.6528-6531.2005) PMID: [15858037](https://pubmed.ncbi.nlm.nih.gov/15858037/)
79. Frost SD, Liu Y, Pond SL, Chappey C, Wrin T, et al. (2005) Characterization of human immunodeficiency virus type 1 (HIV-1) envelope variation and neutralizing antibody responses during transmission of HIV-1 subtype B. *J Virol* 79: 6523–6527. doi: [10.1128/JVI.79.10.6523-6527.2005](https://doi.org/10.1128/JVI.79.10.6523-6527.2005) PMID: [15858036](https://pubmed.ncbi.nlm.nih.gov/15858036/)
 80. Amornkul PN, Karita E, Kamali A, Rida WN, Sanders EJ, et al. (2013) Disease progression by infecting HIV-1 subtype in a seroconverter cohort in sub-Saharan Africa. *AIDS* 27: 2775–2786. doi: [10.1097/QAD.000000000000012](https://doi.org/10.1097/QAD.000000000000012) PMID: [24113395](https://pubmed.ncbi.nlm.nih.gov/24113395/)
 81. Zhang M, Gaschen B, Blay W, Foley B, Haigwood N, et al. (2004) Tracking global patterns of N-linked glycosylation site variation in highly variable viral glycoproteins: HIV, SIV, and HCV envelopes and influenza hemagglutinin. *Glycobiology* 14: 1229–1246. doi: [10.1093/glycob/cwh106](https://doi.org/10.1093/glycob/cwh106) PMID: [15175256](https://pubmed.ncbi.nlm.nih.gov/15175256/)
 82. Wills C, Farmer A, Myers G (1996) Rapid sequon evolution in human immunodeficiency virus type 1 relative to human immunodeficiency virus type 2. *AIDS Res Hum Retroviruses* 12: 1383–1384. doi: [10.1089/aid.1996.12.1383](https://doi.org/10.1089/aid.1996.12.1383) PMID: [8891118](https://pubmed.ncbi.nlm.nih.gov/8891118/)
 83. Kryazhimskiy S, Plotkin JB (2008) The population genetics of dN/dS. *PLoS Genet* 4: e1000304. doi: [10.1371/journal.pgen.1000304](https://doi.org/10.1371/journal.pgen.1000304) PMID: [19081788](https://pubmed.ncbi.nlm.nih.gov/19081788/)
 84. Brandt BW, Feenstra KA, Heringa J (2010) Multi-Hamony: detecting functional specificity from sequence alignment. *Nucleic Acids Res* 38: W35–40. doi: [10.1093/nar/gkq415](https://doi.org/10.1093/nar/gkq415) PMID: [20525785](https://pubmed.ncbi.nlm.nih.gov/20525785/)
 85. Bunnik EM, Euler Z, Welkers MR, Boeser-Nunnink BD, Grijsen ML, et al. (2010) Adaptation of HIV-1 envelope gp120 to humoral immunity at a population level. *Nat Med* 16: 995–997. doi: [10.1038/nm.2203](https://doi.org/10.1038/nm.2203) PMID: [20802498](https://pubmed.ncbi.nlm.nih.gov/20802498/)
 86. van Gils MJ, Bunnik EM, Boeser-Nunnink BD, Burger JA, Terlouw-Klein M, et al. (2011) Longer V1V2 region with increased number of potential N-linked glycosylation sites in the HIV-1 envelope glycoprotein protects against HIV-specific neutralizing antibodies. *J Virol* 85: 6986–6995. doi: [10.1128/JVI.00268-11](https://doi.org/10.1128/JVI.00268-11) PMID: [21593147](https://pubmed.ncbi.nlm.nih.gov/21593147/)
 87. Ferreira CB, Merino-Mansilla A, Llano A, Perez I, Crespo I, et al. (2013) Evolution of Broadly Cross-Reactive HIV-1-Neutralizing Activity: Therapy-Associated Decline, Positive Association with Detectable Viremia, and Partial Restoration of B-Cell Subpopulations. *J Virol* 87: 12227–12236. doi: [10.1128/JVI.02155-13](https://doi.org/10.1128/JVI.02155-13) PMID: [24006439](https://pubmed.ncbi.nlm.nih.gov/24006439/)
 88. Euler Z, van Gils MJ, Boeser-Nunnink BD, Schuitemaker H, van Manen D (2013) Genome-wide association study on the development of cross-reactive neutralizing antibodies in HIV-1 infected individuals. *PLoS One* 8: e54684. doi: [10.1371/journal.pone.0054684](https://doi.org/10.1371/journal.pone.0054684) PMID: [23372753](https://pubmed.ncbi.nlm.nih.gov/23372753/)
 89. Sanders RW, van Gils MJ, Derking R, Sok D, Ketas TJ, et al. (2015) HIV-1 VACCINES. HIV-1 neutralizing antibodies induced by native-like envelope trimers. *Science* 349: aac4223. doi: [10.1126/science.aac4223](https://doi.org/10.1126/science.aac4223) PMID: [26089353](https://pubmed.ncbi.nlm.nih.gov/26089353/)
 90. Crooks ET, Tong T, Chakrabarti B, Narayan K, Georgiev IS, et al. (2015) Vaccine-Elicited Tier 2 HIV-1 Neutralizing Antibodies Bind to Quaternary Epitopes Involving Glycan-Deficient Patches Proximal to the CD4 Binding Site. *PLoS Pathog* 11: e1004932. doi: [10.1371/journal.ppat.1004932](https://doi.org/10.1371/journal.ppat.1004932) PMID: [26023780](https://pubmed.ncbi.nlm.nih.gov/26023780/)
 91. Schulz BE (2012) Beyond the Sequon: Sites of N-Glycosylation. In: Petrescu S, editor. *Glycosylation: InTech*.
 92. Gavel Y, von Heijne G (1990) Sequence differences between glycosylated and non-glycosylated Asn-X-Thr/Ser acceptor sites: implications for protein engineering. *Protein Eng* 3: 433–442. PMID: [2349213](https://pubmed.ncbi.nlm.nih.gov/2349213/)
 93. Kaplan HA, Welply JK, Lennarz WJ (1987) Oligosaccharyl transferase: the central enzyme in the pathway of glycoprotein assembly. *Biochim Biophys Acta* 906: 161–173. PMID: [3297152](https://pubmed.ncbi.nlm.nih.gov/3297152/)
 94. Jenkins N, Parekh RB, James DC (1996) Getting the glycosylation right: implications for the biotechnology industry. *Nat Biotechnol* 14: 975–981. doi: [10.1038/nbt0896-975](https://doi.org/10.1038/nbt0896-975) PMID: [9631034](https://pubmed.ncbi.nlm.nih.gov/9631034/)
 95. Bause E (1984) Model studies on N-glycosylation of proteins. *Biochem Soc Trans* 12: 514–517. PMID: [6428943](https://pubmed.ncbi.nlm.nih.gov/6428943/)
 96. Gerber S, Lizak C, Michaud G, Bucher M, Darbre T, et al. (2013) Mechanism of bacterial oligosaccharyltransferase: in vitro quantification of sequon binding and catalysis. *J Biol Chem* 288: 8849–8861. doi: [10.1074/jbc.M112.445940](https://doi.org/10.1074/jbc.M112.445940) PMID: [23382388](https://pubmed.ncbi.nlm.nih.gov/23382388/)
 97. Shrimal S, Gilmore R (2013) Glycosylation of closely spaced acceptor sites in human glycoproteins. *J Cell Sci* 126: 5513–5523. doi: [10.1242/jcs.139584](https://doi.org/10.1242/jcs.139584) PMID: [24105266](https://pubmed.ncbi.nlm.nih.gov/24105266/)
 98. Bano-Polo M, Baldin F, Tamborero S, Marti-Renom MA, Mingarro I (2011) N-glycosylation efficiency is determined by the distance to the C-terminus and the amino acid preceding an Asn-Ser-Thr sequon. *Protein Sci* 20: 179–186. doi: [10.1002/pro.551](https://doi.org/10.1002/pro.551) PMID: [21082725](https://pubmed.ncbi.nlm.nih.gov/21082725/)

99. Shakin-Eshleman SH, Spitalnik SL, Kasturi L (1996) The amino acid at the X position of an Asn-X-Ser sequon is an important determinant of N-linked core-glycosylation efficiency. *J Biol Chem* 271: 6363–6366. PMID: [8626433](#)
100. Myers G, Lenroot R (1992) HIV glycosylation: what does it portend? *AIDS Res Hum Retroviruses* 8: 1459–1460. doi: [10.1089/aid.1992.8.1459](#) PMID: [1466982](#)
101. Lasky LA, Groopman JE, Fennie CW, Benz PM, Capon DJ, et al. (1986) Neutralization of the AIDS retrovirus by antibodies to a recombinant envelope glycoprotein. *Science* 233: 209–212. PMID: [3014647](#)
102. Wyatt R, Sodroski J (1998) The HIV-1 envelope glycoproteins: fusogens, antigens, and immunogens. *Science* 280: 1884–1888. PMID: [9632381](#)
103. Stewart-Jones GB, Soto C, Lemmin T, Chuang GY, Druz A, et al. (2016) Trimeric HIV-1-Env Structures Define Glycan Shields from Clades A, B, and G. *Cell* 165: 813–826. doi: [10.1016/j.cell.2016.04.010](#) PMID: [27114034](#)
104. Behrens AJ, Vasiljevic S, Pritchard LK, Harvey DJ, Andev RS, et al. (2016) Composition and Antigenic Effects of Individual Glycan Sites of a Trimeric HIV-1 Envelope Glycoprotein. *Cell Rep* 14: 2695–2706. doi: [10.1016/j.celrep.2016.02.058](#) PMID: [26972002](#)
105. Doores KJ, Bonomelli C, Harvey DJ, Vasiljevic S, Dwek RA, et al. (2010) Envelope glycans of immunodeficiency virions are almost entirely oligomannose antigens. *Proc Natl Acad Sci U S A* 107: 13800–13805. doi: [10.1073/pnas.1006498107](#) PMID: [20643940](#)
106. Bonomelli C, Doores KJ, Dunlop DC, Thaney V, Dwek RA, et al. (2011) The glycan shield of HIV is predominantly oligomannose independently of production system or viral clade. *PLoS One* 6: e23521. doi: [10.1371/journal.pone.0023521](#) PMID: [21858152](#)
107. Liu Y, Curlin ME, Diem K, Zhao H, Ghosh AK, et al. (2008) Env length and N-linked glycosylation following transmission of human immunodeficiency virus Type 1 subtype B viruses. *Virology* 374: 229–233. doi: [10.1016/j.virol.2008.01.029](#) PMID: [18314154](#)
108. Gnanakaran S, Bhattacharya T, Daniels M, Keele BF, Hraber PT, et al. (2011) Recurrent signature patterns in HIV-1 B clade envelope glycoproteins associated with either early or chronic infections. *PLoS Pathog* 7: e1002209. doi: [10.1371/journal.ppat.1002209](#) PMID: [21980282](#)
109. Blattner C, Lee JH, Sliepen K, Derking R, Falkowska E, et al. (2014) Structural delineation of a quaternary, cleavage-dependent epitope at the gp41-gp120 interface on intact HIV-1 Env trimers. *Immunity* 40: 669–680. doi: [10.1016/j.immuni.2014.04.008](#) PMID: [24768348](#)
110. Scanlan CN, Pantophlet R, Wormald MR, Saphire EO, Calarese D, et al. (2003) The carbohydrate epitope of the neutralizing anti-HIV-1 antibody 2G12. *Adv Exp Med Biol* 535: 205–218. PMID: [14714897](#)
111. Calarese DA, Scanlan CN, Zwirk MB, Deechongkit S, Mimura Y, et al. (2003) Antibody domain exchange is an immunological solution to carbohydrate cluster recognition. *Science* 300: 2065–2071. doi: [10.1126/science.1083182](#) PMID: [12829775](#)
112. Falkowska E, Le KM, Ramos A, Doores KJ, Lee JH, et al. (2014) Broadly neutralizing HIV antibodies define a glycan-dependent epitope on the prefusion conformation of gp41 on cleaved envelope trimers. *Immunity* 40: 657–668. doi: [10.1016/j.immuni.2014.04.009](#) PMID: [24768347](#)
113. Doores KJ, Kong L, Krumm SA, Le KM, Sok D, et al. (2015) Two classes of broadly neutralizing antibodies within a single lineage directed to the high-mannose patch of HIV envelope. *J Virol* 89: 1105–1118. doi: [10.1128/JVI.02905-14](#) PMID: [25378488](#)
114. Garces F, Sok D, Kong L, McBride R, Kim HJ, et al. (2014) Structural evolution of glycan recognition by a family of potent HIV antibodies. *Cell* 159: 69–79. doi: [10.1016/j.cell.2014.09.009](#) PMID: [25259921](#)
115. Huang J, Kang BH, Pancera M, Lee JH, Tong T, et al. (2014) Broad and potent HIV-1 neutralization by a human antibody that binds the gp41-gp120 interface. *Nature* 515: 138–142. doi: [10.1038/nature13601](#) PMID: [25186731](#)
116. Kong L, Lee JH, Doores KJ, Murin CD, Julien JP, et al. (2013) Supersite of immune vulnerability on the glycosylated face of HIV-1 envelope glycoprotein gp120. *Nat Struct Mol Biol* 20: 796–803. doi: [10.1038/nsmb.2594](#) PMID: [23708606](#)
117. Mouquet H, Scharf L, Euler Z, Liu Y, Eden C, et al. (2012) Complex-type N-glycan recognition by potent broadly neutralizing HIV antibodies. *Proc Natl Acad Sci U S A* 109: E3268–3277. doi: [10.1073/pnas.1217207109](#) PMID: [23115339](#)
118. Pancera M, Yang Y, Louder MK, Gorman J, Lu G, et al. (2013) N332-Directed Broadly Neutralizing Antibodies Use Diverse Modes of HIV-1 Recognition: Inferences from Heavy-Light Chain Complementations of Function. *PLoS One* 8: e55701. doi: [10.1371/journal.pone.0055701](#) PMID: [23431362](#)

119. Pejchal R, Doores KJ, Walker LM, Khayat R, Huang PS, et al. (2011) A potent and broad neutralizing antibody recognizes and penetrates the HIV glycan shield. *Science* 334: 1097–1103. doi: [10.1126/science.1213256](https://doi.org/10.1126/science.1213256) PMID: [21998254](https://pubmed.ncbi.nlm.nih.gov/21998254/)
120. Scharf L, Scheid JF, Lee JH, West AP Jr., Chen C, et al. (2014) Antibody 8ANC195 reveals a site of broad vulnerability on the HIV-1 envelope spike. *Cell Rep* 7: 785–795. doi: [10.1016/j.celrep.2014.04.001](https://doi.org/10.1016/j.celrep.2014.04.001) PMID: [24767986](https://pubmed.ncbi.nlm.nih.gov/24767986/)
121. Walker LM, Phogat SK, Chan-Hui PY, Wagner D, Phung P, et al. (2009) Broad and potent neutralizing antibodies from an African donor reveal a new HIV-1 vaccine target. *Science* 326: 285–289. doi: [10.1126/science.1178746](https://doi.org/10.1126/science.1178746) PMID: [19729618](https://pubmed.ncbi.nlm.nih.gov/19729618/)
122. McLellan JS, Pancera M, Carrico C, Gorman J, Julien JP, et al. (2011) Structure of HIV-1 gp120 V1/V2 domain with broadly neutralizing antibody PG9. *Nature* 480: 336–343. doi: [10.1038/nature10696](https://doi.org/10.1038/nature10696) PMID: [22113616](https://pubmed.ncbi.nlm.nih.gov/22113616/)
123. West AP Jr., Diskin R, Nussenzweig MC, Bjorkman PJ (2012) Structural basis for germ-line gene usage of a potent class of antibodies targeting the CD4-binding site of HIV-1 gp120. *Proc Natl Acad Sci U S A* 109: E2083–2090. doi: [10.1073/pnas.1208984109](https://doi.org/10.1073/pnas.1208984109) PMID: [22745174](https://pubmed.ncbi.nlm.nih.gov/22745174/)
124. Zhou T, Georgiev I, Wu X, Yang ZY, Dai K, et al. (2010) Structural basis for broad and potent neutralization of HIV-1 by antibody VRC01. *Science* 329: 811–817. doi: [10.1126/science.1192819](https://doi.org/10.1126/science.1192819) PMID: [20616231](https://pubmed.ncbi.nlm.nih.gov/20616231/)
125. Scharf L, West AP Jr., Gao H, Lee T, Scheid JF, et al. (2013) Structural basis for HIV-1 gp120 recognition by a germ-line version of a broadly neutralizing antibody. *Proc Natl Acad Sci U S A* 110: 6049–6054. doi: [10.1073/pnas.1303682110](https://doi.org/10.1073/pnas.1303682110) PMID: [23524883](https://pubmed.ncbi.nlm.nih.gov/23524883/)
126. Pritchard LK, Vasiljevic S, Ozorowski G, Seabright GE, Cupo A, et al. (2015) Structural Constraints Determine the Glycosylation of HIV-1 Envelope Trimers. *Cell Rep* 11: 1604–1613. doi: [10.1016/j.celrep.2015.05.017](https://doi.org/10.1016/j.celrep.2015.05.017) PMID: [26051934](https://pubmed.ncbi.nlm.nih.gov/26051934/)
127. Sharma SK, de Val N, Bale S, Guenaga J, Tran K, et al. (2015) Cleavage-independent HIV-1 Env trimers engineered as soluble native spike mimetics for vaccine design. *Cell Rep* 11: 539–550. doi: [10.1016/j.celrep.2015.03.047](https://doi.org/10.1016/j.celrep.2015.03.047) PMID: [25892233](https://pubmed.ncbi.nlm.nih.gov/25892233/)
128. Guenaga J, Dubrovskaya V, de Val N, Sharma SK, Carrette B, et al. (2016) Structure guided redesign increases the propensity of HIV Env to generate highly stable soluble trimers. *Journal of Virology* 90: 2806–2817.
129. Sanders RW, Derking R, Cupo A, Julien JP, Yasmeen A, et al. (2013) A next-generation cleaved, soluble HIV-1 Env trimer, BG505 SOSIP.664 gp140, expresses multiple epitopes for broadly neutralizing but not non-neutralizing antibodies. *PLoS Pathog* 9: e1003618. doi: [10.1371/journal.ppat.1003618](https://doi.org/10.1371/journal.ppat.1003618) PMID: [24068931](https://pubmed.ncbi.nlm.nih.gov/24068931/)
130. Pugach P, Ozorowski G, Cupo A, Ringe R, Yasmeen A, et al. (2015) A native-like SOSIP.664 trimer based on an HIV-1 subtype B env gene. *J Virol* 89: 3380–3395. doi: [10.1128/JVI.03473-14](https://doi.org/10.1128/JVI.03473-14) PMID: [25589637](https://pubmed.ncbi.nlm.nih.gov/25589637/)
131. Julien JP, Lee JH, Ozorowski G, Hua Y, Torrents de la Pena A, et al. (2015) Design and structure of two HIV-1 clade C SOSIP.664 trimers that increase the arsenal of native-like Env immunogens. *Proc Natl Acad Sci U S A* 112: 11947–11952. doi: [10.1073/pnas.1507793112](https://doi.org/10.1073/pnas.1507793112) PMID: [26372963](https://pubmed.ncbi.nlm.nih.gov/26372963/)
132. Hessell AJ, Malherbe DC, Pissani F, McBurney S, Krebs SJ, et al. (2016) Achieving Potent Autologous Neutralizing Antibody Responses against Tier 2 HIV-1 Viruses by Strategic Selection of Envelope Immunogens. *Journal of Immunology*.
133. Malherbe DC, Pissani F, Sather DN, Guo B, Pandey S, et al. (2014) Envelope variants circulating as initial neutralization breadth developed in two HIV-infected subjects stimulate multiclade neutralizing antibodies in rabbits. *J Virol* 88: 12949–12967. doi: [10.1128/JVI.01812-14](https://doi.org/10.1128/JVI.01812-14) PMID: [25210191](https://pubmed.ncbi.nlm.nih.gov/25210191/)
134. Malherbe DC, Doria-Rose NA, Misher L, Beckett T, Puryear WB, et al. (2011) Sequential immunization with a subtype B HIV-1 envelope quasispecies partially mimics the in vivo development of neutralizing antibodies. *J Virol* 85: 5262–5274. doi: [10.1128/JVI.02419-10](https://doi.org/10.1128/JVI.02419-10) PMID: [21430056](https://pubmed.ncbi.nlm.nih.gov/21430056/)
135. Pissani F, Malherbe DC, Robins H, DeFilippis VR, Park B, et al. (2012) Motif-optimized subtype A HIV envelope-based DNA vaccines rapidly elicit neutralizing antibodies when delivered sequentially. *Vaccine* 30: 5519–5526. doi: [10.1016/j.vaccine.2012.06.042](https://doi.org/10.1016/j.vaccine.2012.06.042) PMID: [22749601](https://pubmed.ncbi.nlm.nih.gov/22749601/)
136. Kilgore KM, Murphy MK, Burton SL, Wetzel KS, Smith SA, et al. (2015) Characterization and Implementation of a Diverse Simian Immunodeficiency Virus SIVsm Envelope Panel in the Assessment of Neutralizing Antibody Breadth Elicited in Rhesus Macaques by Multimodal Vaccines Expressing the SIVmac239 Envelope. *J Virol* 89: 8130–8151. doi: [10.1128/JVI.01221-14](https://doi.org/10.1128/JVI.01221-14) PMID: [26018167](https://pubmed.ncbi.nlm.nih.gov/26018167/)
137. Tang H, Robinson JE, Gnanakaran S, Li M, Rosenberg ES, et al. (2011) Epitopes immediately below the base of the V3 loop of gp120 as targets for the initial autologous neutralizing antibody response in two HIV-1 subtype B-infected individuals. *J Virol* 85: 9286–9299. doi: [10.1128/JVI.02286-10](https://doi.org/10.1128/JVI.02286-10) PMID: [21734041](https://pubmed.ncbi.nlm.nih.gov/21734041/)

138. Gao F, Bonsignori M, Liao HX, Kumar A, Xia SM, et al. (2014) Cooperation of B cell lineages in induction of HIV-1-broadly neutralizing antibodies. *Cell* 158: 481–491. doi: [10.1016/j.cell.2014.06.022](https://doi.org/10.1016/j.cell.2014.06.022) PMID: [25065977](https://pubmed.ncbi.nlm.nih.gov/25065977/)
139. Jardine JG, Kulp DW, Havenar-Daughton C, Sarkar A, Briney B, et al. (2016) HIV-1 broadly neutralizing antibody precursor B cells revealed by germline-targeting immunogen. *Science* 351: 1458–1463. doi: [10.1126/science.aad9195](https://doi.org/10.1126/science.aad9195) PMID: [27013733](https://pubmed.ncbi.nlm.nih.gov/27013733/)
140. Jardine J, Julien JP, Menis S, Ota T, Kalyuzhnyi O, et al. (2013) Rational HIV immunogen design to target specific germline B cell receptors. *Science* 340: 711–716. doi: [10.1126/science.1234150](https://doi.org/10.1126/science.1234150) PMID: [23539181](https://pubmed.ncbi.nlm.nih.gov/23539181/)
141. Price MA, Wallis CL, Lakhi S, Karita E, Kamali A, et al. (2011) Transmitted HIV type 1 drug resistance among individuals with recent HIV infection in East and Southern Africa. *AIDS Res Hum Retroviruses* 27: 5–12. doi: [10.1089/aid.2010.0030](https://doi.org/10.1089/aid.2010.0030) PMID: [21091377](https://pubmed.ncbi.nlm.nih.gov/21091377/)
142. Tang J, Malhotra R, Song W, Brill I, Hu L, et al. (2010) Human leukocyte antigens and HIV type 1 viral load in early and chronic infection: predominance of evolving relationships. *PLoS One* 5: e9629. doi: [10.1371/journal.pone.0009629](https://doi.org/10.1371/journal.pone.0009629) PMID: [20224785](https://pubmed.ncbi.nlm.nih.gov/20224785/)
143. Yue L, Pfafferoth KJ, Baalwa J, Conrod K, Dong CC, et al. (2015) Transmitted virus fitness and host T cell responses collectively define divergent infection outcomes in two HIV-1 recipients. *PLoS Pathog* 11: e1004565. doi: [10.1371/journal.ppat.1004565](https://doi.org/10.1371/journal.ppat.1004565) PMID: [25569444](https://pubmed.ncbi.nlm.nih.gov/25569444/)
144. Lynch RM, Rong R, Li B, Shen T, Honnen W, et al. (2010) Subtype-specific conservation of isoleucine 309 in the envelope V3 domain is linked to immune evasion in subtype C HIV-1 infection. *Virology*.
145. Giorgi EE, Bhattacharya T (2012) A note on two-sample tests for comparing intra-individual genetic sequence diversity between populations. *Biometrics* 68: 1323–1326; author reply 1326. doi: [10.1111/j.1541-0420.2012.01775.x](https://doi.org/10.1111/j.1541-0420.2012.01775.x) PMID: [23004569](https://pubmed.ncbi.nlm.nih.gov/23004569/)
146. Archary D, Rong R, Gordon ML, Boliar S, Madiga M, et al. (2012) Characterization of anti-HIV-1 neutralizing and binding antibodies in chronic HIV-1 subtype C infection. *Virology* Accepted.
147. Li B, Stefano-Cole K, Kuhrt DM, Gordon SN, Else JG, et al. (2010) Nonpathogenic simian immunodeficiency virus infection of sooty mangabeys is not associated with high levels of autologous neutralizing antibodies. *J Virol* 84: 6248–6253. doi: [10.1128/JVI.00295-10](https://doi.org/10.1128/JVI.00295-10) PMID: [20375163](https://pubmed.ncbi.nlm.nih.gov/20375163/)
148. Ortiz AM, Klatt NR, Li B, Yi Y, Tabb B, et al. (2011) Depletion of CD4(+) T cells abrogates post-peak decline of viremia in SIV-infected rhesus macaques. *J Clin Invest* 121: 4433–4445. doi: [10.1172/JCI46023](https://doi.org/10.1172/JCI46023) PMID: [22005304](https://pubmed.ncbi.nlm.nih.gov/22005304/)
149. Rong R, Bibollet-Ruche F, Mulenga J, Allen S, Blackwell JL, et al. (2007) Role of V1V2 and other human immunodeficiency virus type 1 envelope domains in resistance to autologous neutralization during clade C infection. *J Virol* 81: 1350–1359. doi: [10.1128/JVI.01839-06](https://doi.org/10.1128/JVI.01839-06) PMID: [17079307](https://pubmed.ncbi.nlm.nih.gov/17079307/)
150. Rong R, Gnanakaran S, Decker JM, Bibollet-Ruche F, Taylor J, et al. (2007) Unique Mutational Patterns in the Envelope {alpha}2 Amphipathic Helix and Acquisition of Length in gp120 Hyper-variable Domains are Associated with Resistance to Autologous Neutralization of Subtype C Human Immunodeficiency Virus type 1. *J Virol* 81: 5658–5668. doi: [10.1128/JVI.00257-07](https://doi.org/10.1128/JVI.00257-07) PMID: [17360739](https://pubmed.ncbi.nlm.nih.gov/17360739/)